RESEARCH ARTICLE

MycoKeys
A peer-reviewed open-access journal
Launched to accelerate biodiversity research

New polyketides from the liquid culture of *Diaporthe breyniae* sp. nov. (Diaporthales, Diaporthaceae)

Blondelle Matio Kemkuignou[1,2], Lena Schweizer[1], Christopher Lambert[1,2],
Elodie Gisèle M. Anoumedem[3], Simeon F. Kouam[3],
Marc Stadler[1,2], Yasmina Marin-Felix[1,2]

1 *Department of Microbial Drugs, Helmholtz Centre for Infection Research (HZI) and German Centre for Infection Research (DZIF), Partner Site Hannover/Braunschweig, Inhoffenstrasse 7, 38124 Braunschweig, Germany* **2** *Institute of Microbiology, Technische Universität Braunschweig, Spielmannstraße 7, 38106 Braunschweig, Germany* **3** *Department of Chemistry, Higher Teacher Training College, University of Yaoundé I, Yaoundé P.O. Box 47, Cameroon*

Corresponding author: *Yasmina Marin Felix (Yasmina.marinfelix@helmholtz-hzi.de)*

Abstract

During the course of a study on the biodiversity of endophytes from Cameroon, a fungal strain was isolated. A multigene phylogenetic inference using five DNA loci revealed that this strain represents an undescribed species of *Diaporthe*, which is introduced here as *D. breyniae*. Investigation into the chemistry of this fungus led to the isolation of two previously undescribed secondary metabolites for which the trivial names fusaristatins G (**7**) and H (**8**) are proposed, together with eleven known compounds. The structures of all of the metabolites were established by using one-dimensional (1D) and two-dimensional (2D) Nuclear Magnetic Resonance (NMR) spectroscopic data in combination with High-Resolution Electro-Spray Ionization Mass Spectrometry (HR-ESIMS) data. The absolute configuration of phomopchalasin N (**4**), which was reported for the first time concurrently to the present publication, was determined by analysis of its Rotating frame Overhauser Effect SpectroscopY (ROESY) spectrum and by comparison of its Electronic Circular Dichroism (ECD) spectrum with that of related compounds. A selection of the isolated secondary metabolites were tested for antimicrobial and cytotoxic activities, and compounds **4** and **7** showed weak antifungal and antibacterial activity. On the other hand, compound **4** showed moderate cytotoxic activity against all tested cancer cell lines with IC_{50} values in the range of 5.8–45.9 μM. The latter was found to be less toxic than the other isolated cytochalasins (**1–3**) and gave hints in regards to the structure-activity relationship (SAR) of the studied cytochalasins. Fusaristatin H (**8**) also exhibited weak cytotoxicity against KB3.1 cell lines with an IC_{50} value of 30.3 μM.

Graphical abstract

Diaporthe breyniae
sp. nov.
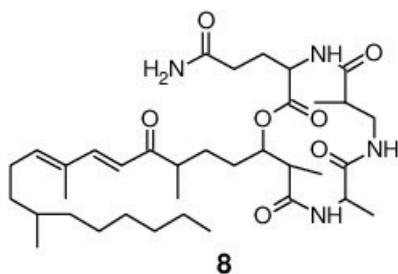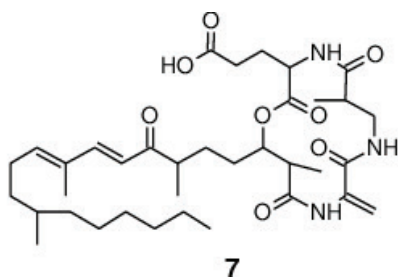
Introduction

The genus *Diaporthe* (including their asexual states, which were previously referred to as *Phomopsis* spp.) comprises several hundred species mostly attributed to plant pathogens, non-pathogenic endophytes, or saprobes in terrestrial host plants (Chepkirui and Stadler 2017; Xu et al. 2021). The term "endophytic fungi" herein refers to a group of microorganisms that inhabit the internal parts of a plant, but typically cause no apparent symptoms of disease in the host plant (Stone et al. 2000). Fungal endophytes belonging to the genus *Diaporthe* have been widely investigated by natural product chemists and have proven to be a rich source of novel organic compounds with interesting biological activities and a high level of chemical diversity (Chepkirui and Stadler 2017). They have been shown to predominantly produce polyketides, but PKS/NRPS-derived hybrids like cytochalasins have also been frequently reported from *Diaporthe* (Jouda et al. 2016; Chepkirui and Stadler 2017). Initially, cytochalasins have been discovered for their potent cytotoxic effects, which are due to their interference with the actin cytoskeleton (Yahara et al. 1982) and have been targeted primarily as anticancer agents. However, not all cytochalasins are equally active on actin (Kretz et al. 2019), and they were even found to significantly inhibit biofilm formation of an important human pathogenic bacterium (Yuyama et al. 2018). The current paper supports the activities of an interdisciplinary consortium that aims at exploring the

chemical space of the cytochalasins, in order to establish structure-activity relationships (SAR) and systematically explore their utility for application in various medical applications. Owing to the structural complexity of cytochalasins, their total synthesis remains tedious and requires several reaction steps with relatively low final yields (Zaghouani et al. 2016; Long et al. 2018). Moreover, most of the compounds that were reported previously have not been studied thoroughly for their biological effects; hence, it is worth obtaining them from the fungal producer organisms by *de novo* isolation and characterization.

We have recently isolated and studied a new endophytic species of *Diaporthe* from the twigs of *Breynia oblongifolia*. We noted prominent antimicrobial effects in the extracts derived from this strain and decided to study its secondary metabolites. The current paper includes the description of the new species *D. breyniae* sp. nov., and reports details on the isolation and structure elucidation of its secondary metabolites, as well as an account of their biological properties.

Materials and methods

Fungal isolation

The fungus was isolated from fresh twigs of an apparently healthy plant belonging to *Breynia oblongifolia* in Kala Mountain (Yaoundé, Cameroon). Fresh twigs (5 × 5 cm length) of *Breynia oblongifolia* were thoroughly washed with running tap water, then disinfected in 75% ethanol for 1 min, in 3% sodium hypochlorite (NaClO) for 10 min, and finally in 75% ethanol for 30 s. These twigs were then rinsed three times in sterile distilled water and dried on sterile tissue paper under a laminar flow hood. Small segments of the twigs were transferred to Petri dishes containing potato dextrose agar (PDA, HiMedia, Mumbai, India) supplemented with 100 mg/mL penicillin and 100 µg/mL streptomycin sulphate and incubated at 28 °C. After 10 days, fungal colonies were examined and hyphal tips were transferred to PDA using a sterile needle and incubated at 28 °C.

Herbarium type material and the ex-type strain of the new species are maintained at the collection of the Westerdijk Fungal Biodiversity Institute (CBS), Utrecht, the Netherlands.

Phenotypic study

For cultural characterization, the isolate was grown for 15 days on malt extract agar (MEA; HiMedia, Mumbai, India), oatmeal agar (OA; Sigma-Aldrich, St. Louis, Missouri, USA), and PDA at 21 °C in darkness (Guarnaccia et al. 2018). Color notations in parentheses are taken from the color chart of The Royal Horticultural Society London (1966). The fungus was grown in 2% tap water agar supplemented with sterile pine needles (PNA; Smith et al. 1996) to induce sporulation.

Molecular study

DNA of the fungus was extracted and purified directly from colony growing in yeast malt agar (YM agar; malt extract 10 g/L, yeast extract 4 g/L, D-glucose 4 g/L, agar 20 g/L, pH 6.3 before autoclaving), following the Fungal gDNA Miniprep Kit EZ-10 Spin Column protocol (NBS Biologicals, Cambridgeshire, UK). The amplification of the ITS, *cal*, *his3*, *tef1* and *tub2* loci were performed according to White et al. (1990) (ITS), Carbone and Kohn (1999) (*cal* and *tef1*), Glass and Donaldson (1995) (*his3* and *tub2*) and Crous et al. (2004) (*his3*). PCR products were purified and sequenced using Sanger Cycle Sequencing method at Microsynth Seqlab GmbH (Göttingen, Germany), and the consensus sequences obtained employing the de-novo assembly feature of the Geneious 7.1.9 (http://www.geneious.com, Kearse et al. 2012) program package using a forward and reverse read.

In order to restrict the phylogenetic inference to the relevant species to compare with, a first phylogenetic analysis was carried out based on the combination of the five loci sequences (ITS, *cal*, *his3*, *tef1*, *tub2*) of our isolate and a selection of sequence data derived from type material or reference strains from all *Diaporthe* spp. available in NCBI. Each locus was aligned separately using MAFFT v. 7.017 (algorithm G-INS-I, gap open penalty set to 1.53, offset value 0.123 with options set for automatically determining sequence direction automatically and more accurately) as available as a Geneious 7.1.9 plugin (Katoh and Standley 2013) and manually adjusted in MEGA v. 10.2.4 (Kumar et al. 2018). Alignment errors were minimized by using gblocks (Talavera and Castresana 2007); with options set for allowed block positions 'with half', minimum length of a block set to 5 and a maximum of 10 contiguous nonconserved positions) and concatenated by employing the phylosuite v 1.2.2 program package (Zhang et al. 2020). Maximum-Likelihood tree inference followed using IQTree V2.1.3 (Minh et al. 2020) preceded by calculation and automatic selection of the appropriate nucleotide exchange model using ModelFinder (Chernomor et al. 2016; Kalyaanamoorthy et al. 2017) based on Bayesian inference criterion. Bootstrap support was calculated by parallelizing 10 independent maximum-likelihood (ML) tree searches with 100 bootstrap replicates each to minimize computational burden. The total 1000 bootstrap replicates were consequently mapped onto the ML tree with the best (highest) ML score. After selection of the core group related to the sequences derived from *D. breyniae* sp. nov., a second phylogenetic analysis was performed including all five sequenced loci, using *D. amygdali* CBS 126679[T] and *D. eres* CBS 138594[T] as outgroups. Sequence alignment and curation steps were identical, with exemption of a manual curation instead of employing automatic filtering for misaligned alignment sections using gblocks. ML trees using the supermatrix and single loci, respectively, were inferred using IQTree 2.1.3 with ModelFinder to determine optimal substitution models for each loci and partition, using 1000 bootstrap replicates to assign statistical support. The clade in which the sequences of the novel strain clustered, was checked visually for congruence among the single locus trees. Concurrently, a second tree was

inferred following a Bayesian approach using MrBayes 3.2.7a (Ronquist et al. 2012) with nucleotide substitution models previously determined using PartitionFinder2 (Lanfear et al. 2016, options set for unlinked partitions, BIC, restricting models for Bayesian inference) and concatenated in Phylosuite V.1.2.2. Bayesian inference was done in Mr. Bayes v. 3.2.7 (Ronquist et al. 2012), using Markov Chain Monte Carlo (MCMC) with four incrementally heated chains (temperature parameter set to 0.15), starting from a random tree topology. Generations were set to 100.000.000 with convergence controlled by average standard deviation of split frequencies arriving below 0.01. Trees were sampled every 1000 generations with the first 25% of saved trees treated as "burn-in" phase. Posterior probabilities were mapped using the remaining trees. Bootstrap support (bs) ≥ 70 and posterior probability values (pp) ≥ 0.95 were considered significant (Alfaro et al. 2003). The sequences generated in this study are deposited in GenBank (Table 1) and the alignments used in the phylogenetic analysis are included in Supplementary material. Sequences retrieved from GenBank are indicated in Table 1 and Suppl. material 1: S4.

Chromatography and spectral methods

Electrospray ionization mass (ESIMS) spectra were recorded with an UltiMate 3000 Series uHPLC (Thermo Fischer Scientific, Waltman, MA, USA) utilizing a C18 Acquity UPLC BEH column (2.1 × 50 mm, 1.7 µm; Waters, Milford, USA) connected to an amaZon speed ESI-Iontrap-MS (Bruker, Billerica, MA, USA). HPLC parameters were set as follows: solvent A: H_2O + 0.1% formic acid, solvent B: acetonitrile (ACN) + 0.1% formic acid, gradient: 5% B for 0.5 min increasing to 100% B in 19.5 min, then isocratic condition at 100% B for 5 min, a flow rate of 0.6 mL/min, and Diode-Array Detection (DAD) of 210 nm and 190–600 nm.

High-resolution electrospray ionization mass spectrometry (HR-ESIMS) spectra were recorded with an Agilent 1200 Infinity Series HPLC-UV system (Agilent Technologies, Santa Clara, USA; column 2.1 × 50 mm, 1.7 µm, C18 Acquity UPLC BEH (waters), solvent A: H_2O +0.1% formic acid; solvent B: ACN + 0.1% formic acid, gradient: 5% B for 0.5 min increasing to 100% B in 19.5 min and then maintaining 100% B for 5 min, flow rate 0.6 mL/min, UV/Vis detection 200–640 nm) connected to a MaXis ESI-TOF mass spectrometer (Bruker) (scan range 100–2500 *m/z*, capillary voltage 4500 V, dry temperature 200 °C).

Optical rotations were recorded in methanol (Uvasol, Merck, Darmstadt, Germany) by using an Anton Paar MCP-150 polarimeter (Seelze, Germany) at 20 °C. UV/Vis spectra were recorded using methanol (Uvasol, Merck, Darmstadt, Germany) with a Shimadzu UV/Vis 2450 spectrophotometer (Kyoto, Japan). ECD spectra were obtained on a J-815 spectropolarimeter (JASCO, Pfungstadt, Germany). Nuclear magnetic resonance (NMR) spectra were recorded at a temperature of 298 K with an Avance III 500 spectrometer (Bruker, Billerica, MA/USA, ^{1}H-NMR: 500 MHz and ^{13}C-NMR: 125 MHz) and an Ascend 700 spectrometer with 5 mm TCI cryoprobe (Bruker, Billerica, MA/USA, ^{1}H-NMR: 700 MHz and ^{13}C-NMR: 175 MHz).

Table 1. Isolated and reference strains of *Diaporthe* included in this study. # GenBank accession numbers in **bold** were newly generated in this study. The taxonomic novelty is indicated in ***bold italic***.

Species	Isolates[1]	GenBank accession numbers[2]					References
		ITS	*tub2*	*his3*	*tef1*	*cal*	
Diaporthe acaciarum	CBS 138862[T]	KP004460	KP004509	KP004504	-	-	Crous et al. (2014)
D. acericola	MFLUCC 17-0956[T]	KY964224	KY964074	-	KY964180	KY964137	Dissanayake et al. (2017)
D. alangii	CFCC 52556[T]	MH121491	MH121573	MH121451	MH121533	MH121415	Yang et al. (2018)
D. ambigua	CBS 114015[T]	KC343010	KC343978	KC343494	KC343736	KC343252	Gomes et al. (2013)
D. amygdali	CBS 126679[T]	KC343022	KC343990	KC343506	KC343748	KC343264	Gomes et al. (2013)
D. angelicae	CBS 111592[T]	KC343026	KC343994	KC343511	KC343752	KC343268	Gomes et al. (2013)
D. arctii	CBS 136.25	KC343031	KC343999	KC343515	KC343757	KC343273	Gomes et al. (2013)
D. arezzoensis	MFLU 19-2880[T]	MT185503	MT454055	-	-	-	Li et al. (2020)
D. batatas	CBS 122.21	KC343040	KC344008	KC343524	KC343766	KC343282	Gomes et al. (2013)
D. beilharziae	BRIP 54792[T]	JX862529	KF170921	-	JX862535	-	Thompson et al. (2015)
D. biguttulata	ICMP 20657[T]	KJ490582	KJ490403	KJ490524	KJ490461	-	Huang et al. (2015)
D. breyniae	CBS 148910[T]	**ON400846**	**ON409186**	**ON409187**	**ON409188**	**ON409189**	Present study
D. camporesii	JZB 320143[T]	MN533805	MN561316	-	-	-	Hyde et al. (2020)
D. caryae	CFCC 52563[T]	MH121498	MH121580	MH121458	MH121540	MH121422	Yang et al. (2018)
D. celtidis	NCYU 19-0357[T]	MW114346	MW148266	-	MW192209	-	Tennakoon et al. (2021)
D. cerradensis	CMRP 4331[T]	MN173198	MW751671	MW751663	MT311685	MW751655	Iantas et al. (2021)
D. chimonanthi	SCHM 3614[T]	AY622993					Chang et al. (2005)
D. chinensis	MFLUCC 19-0101[T]	MW187324	MW245013		MW205017	MW294199	de Silva et al. (2021)
D. chromolaenae	MFLUCC 17-1422[T]	MH094275	-	-	-	-	Mapook et al. (2020)
D. cichorii	MFLUCC 17-1023[T]	KY964220	KY964104	-	KY964176	KY964133	Dissanayake et al. (2017)
D. cinnamomi	CFCC 52569[T]	MH121504	MH121586	MH121464	MH121546	-	Yang et al. (2018)
D. citriasiana	CBS 134240[T]	JQ954645	KC357459	MF418282	JQ954663	KC357491	Huang et al. (2013)
D. compacta	LC3083[T]	KP267854	KP293434	KP293508	KP267928	-	Gao et al. (2016)
D. convolvuli	CBS 124654	KC343054	KC344022	KC343538	KC343780	KC343296	Gomes et al. (2013)
D. cucurbitae	DAOM 42078[T]	KM453210	KP118848	KM453212	KM453211	-	Udayanga et al. (2015)
D. cuppatea	CBS 117499[T]	AY339322	JX275420	KC343541	AY339354	JX197414	Van Rensburg et al. (2006)
D. discoidispora	ICMP 20662[T]	KJ490624	KJ490445	KJ490566	KJ490503	-	Huang et al. (2015)
D. durionigena	VTCC 930005[T]	MN453530	MT276159	-	MT276157	-	Crous et al. (2020)
D. endophytica	CBS 133811[T]	KC343065	KC344033	KC343549	KC343791	KC343307	Gomes et al. (2013)
D. eres	CBS 138594[T]	KJ210529	KJ420799	KJ420850	KJ210550	KJ434999	Udayanga et al. (2014)
D. fici-septicae	MFLU 18-2588[T]	MW114348	MW148268	-	MW192211	-	Tennakoon et al. (2021)
D. fructicola	MAFF 246408[T]	LC342734	LC342736	LC342737	LC342735	LC342738	Crous et al. (2019)
D. ganjae	CBS 180.91[T]	KC343112	KC344080	KC343596	KC343838	KC343354	Gomes et al. (2013)
D. glabrae	SCHM 3622[T]	AY601918	-	-	-	-	Chang et al. (2005)
D. goulteri	BRIP 55657a[T]	KJ197290	KJ197270	-	KJ197252	-	Thompson et al. (2015)

Species	Isolates[1]	GenBank accession numbers[2]					References
		ITS	*tub2*	*his3*	*tef1*	*cal*	
D. guangdongensis	ZHKUCC20-0014[T]	MT355684	MT409292	-	MT409338	MT409314	Dong et al. (2021)
D. gulyae	BRIP 54025[T]	JF431299	KJ197271	-	JN645803	-	Thompson et al. (2015)
D. guttulata	CGMCC 3.20100[T]	MT385950	MT424705	MW022491	MT424685	MW022470	Dissanayake et al. (2020)
D. helianthi	CBS 592.81[T]	KC343115	KC344083	KC343599	KC343841	JX197454	Gomes et al. (2013)
D. heterostemmatis	SAUCC 194.85[T]	MT822613	MT855810	MT855581	MT855925	MT855692	Sun et al. (2021)
D. hordei	CBS 481.92	KC343120	KC344088	KC343604	KC343846	KC343362	Gomes et al. (2013)
D. hubeiensis	JZB 320123[T]	MK335809	MK500148	-	MK523570	MK500235	Manawasinghe et al. 2019
D. infecunda	CBS 133812[T]	KC343126	KC344094	KC343610	KC343852	KC343368	Gomes et al. (2013)
D. infertilis	CBS 230.52[T]	KC343052	KC344020	KC343536	KC343778	KC343294	Guarnaccia and Crous (2017)
D. kochmanii	BRIP 54033[T]	JF431295	-	-	JN645809	-	Thompson et al. (2011)
D. kongii	BRIP 54031[T]	JF431301	KJ197272	-	JN645797	-	Thompson et al. (2011)
D. leucospermi	CBS 111980[T]	JN712460	KY435673	KY435653	KY435632	KY435663	Crous et al. (2011c)
D. longicolla	FAU 599[T]	KJ590728	KJ610883	KJ659188	KJ590767	KJ612124	Udayanga et al. (2015)
D. longispora	CBS 194.36[T]	KC343135	KC344103	KC343619	KC343861	KC343377	Gomes et al. (2013)
D. lusitanicae	CBS 123212[T]	KC343136	KC344104	KC343620	KC343862	KC343378	Gomes et al. (2013)
D. machili	SAUCC 194.111[T]	MT822639	MT855836	MT855606	MT855951	MT855718	Huang et al. (2021)
D. manihotia	CBS 505.76	KC343138	KC344106	KC343622	KC343864	KC343380	Gomes et al. (2013)
D. masirevicii	BRIP 57892a[T]	KJ197277	KJ197257	-	KJ197239	-	Thompson et al. (2015)
D. mayteni	CBS 133185[T]	KC343139	KC344107	KC343623	KC343865	KC343381	Gomes et al. (2013)
D. megalospora	CBS 143.27	KC343140	KC344108	KC343624	KC343866	KC343382	Gomes et al. (2013)
D. melonis	CBS 507.78[T]	KC343142	KC344110	KC343626	KC343868	KC343384	Gomes et al. (2013)
D. micheliae	SCHM 3603	AY620820	-	-	-	-	Chang et al. (2005)
D. middletonii	BRIP 54884e[T]	KJ197286	KJ197266	-	KJ197248	-	Thompson et al. (2015)
D. myracrodruonis	URM 7972[T]	MK205289	MK205291	-	MK213408	MK205290	da Silva et al. (2019)
D. neoarctii	CBS 109490	KC343145	KC344113	KC343629	KC343871	KC343387	Gomes et al. (2013)
D. neoraonikayaporum	MFLUCC 14-1136[T]	KU712449	KU743988		KU749369	KU749356	Doilom et al. (2017)
D. novem	CBS 127271[T]	KC343157	KC344125	KC343641	KC343883	KC343399	Gomes et al. (2013)
D. ovalispora	ICMP 20659[T]	KJ490628	KJ490449	KJ490570	KJ490507	-	Huang et al. (2015)
D. pachirae	COAD 2074[T]	MG559537	MG559541	-	MG559539	MG559535	Milagres et al. (2018)
D. passifloricola	CBS 141329[T]	KX228292	KX228387	KX228367	-	-	Crous et al. (2016)
D. phaseolorum	CBS 113425	KC343174	KC344142	KC343658	KC343900	KC343416	Gomes et al. (2013)
D. pseudolongicolla	CBS 117165[T]	DQ286285	-	-	DQ286259	-	Petrović et al. (2018)
D. pyracanthae	CBS142384[T]	KY435635	KY435666	KY435645	KY435625	KY435656	Santos et al. (2017)
D. racemosae	CBS 143770[T]	MG600223	MG600227	MG600221	MG600225	MG600219	Marin-Felix et al. (2019)
D. raonikayaporum	CBS 133182[T]	KC343188	KC344156	KC343672	KC343914	KC343430	Gomes et al. (2013)
D. rosae	MFLUCC 17-2658[T]	MG828894	MG843878	-	-	MG829273	Wanasinghe et al. (2018)
D. rosiphthora	COAD 2913[T]	MT311196	-	-	MT313692	MT313690	Pereira et al. (2021)
D. rossmaniae	CAA 762[T]	MK792290	MK837914	MK871432	MK828063	MK883822	Hilário et al. (2020)
D. sackstonii	BRIP 54669b[T]	KJ197287	KJ197267	-	KJ197249	-	Thompson et al. (2015)
D. sambucusii	CFCC 51986[T]	KY852495	KY852511	KY852503	KY852507	KY852499	Yang et al. (2018)

Species	Isolates[1]	GenBank accession numbers[2]					References
		ITS	*tub2*	*his3*	*tef1*	*cal*	
D. schini	CBS 133181[T]	KC343191	KC344159	KC343675	KC343917	KC343433	Gomes et al. (2013)
D. schoeni	MFLU 15-1279[T]	KY964226	KY964109	-	KY964182	KY964139	Dissanayake et al. (2017a)
D. sclerotioides	CBS 296.67[T]	KC343193	KC344161	KC343677	KC343919	KC343435	Gomes et al. (2013)
D. serafiniae	BRIP 55665a[T]	KJ197274	KJ197254		KJ197236	-	Thompson et al. (2015)
D. siamensis	MFLUCC 10-0573a	JQ619879	JX275429	-	JX275393	-	Udayanga et al. (2012)
D. sinensis	CGMCC 3.19521[T]	MK637451	MK660447	-	MK660449	-	Feng et al. (2019)
D. sojae	CBS 139282[T]	KJ590719	KJ610875	KJ659208	KJ590762	KJ612116	Udayanga et al. (2015)
D. stewartii	CBS 193.36	FJ889448	-	-	GQ250324	-	Santos et al. (2010)
D. subellipicola	KUMCC 17-0153[T]	MG746632	MG746634	-	MG746633	-	Hyde et al. (2018)
D. subordinaria	CBS 101711	KC343213	KC344181	KC343697	KC343939	KC343455	Gomes et al. (2013)
D. tecomae	CBS 100547	KC343215	KC344183	KC343699	KC343941	KC343457	Gomes et al.(2013)
D. tectonae	MFLUCC 12-0777[T]	KU712430	KU743977	-	KU749359	KU749345	Doilom et al. (2017)
D. tectonendophytica	MFLUCC 13-0471[T]	KU712439	KU743986	-	KU749367	KU749354	Doilom et al. (2017)
D. terebinthifolii	CBS 133180[T]	KC343216	KC344184	KC343700	KC343942	KC343458	Gomes et al. (2013)
D. thunbergiicola	MFLUCC 12-0033[T]	KP715097	-		KP715098	-	Liu et al. (2015)
D. tulliensis	BRIP 62248a	KR936130	KR936132	-	KR936133	-	Crous et al. (2015)
D. ueckeri	FAU 656	KJ590726	KJ610881	KJ659215	KJ590747	KJ612122	Huang et al. (2015)
	BRIP 54736j (type of *D. miriciae*)	KJ197283	KJ197263	-	KJ197245	-	Thompson et al. (2015)
D. unshiuensis	CGMCC 3.17569[T]	KJ490587	KJ490408	KJ490529	KJ490466		Huang et al. (2015)
D. vexans	CBS 127.14	KC343229	KC344197	KC343713	KC343955	KC343471	Gomes et al.(2013)
D. vitimegaspora	STE-U 2675	AF230749	-	-	-	-	Mostert et al. (2001)
D. vochysiae	LGMF 1583[T]	MG976391	MK007527	MK033323	MK007526	MK007528	Noriler et al. (2019)
D. yunnanensis	CGMCC 3.18289[T]	KX986796	KX999228	KX999267	KX999188	KX999290	Gao et al. (2017)

[1]BRIP: Queensland Plant Pathology Herbarium, Brisbane, Australia; CBS: Westerdijk Fungal Biodiversity Institute, Utrecht, the Netherlands; CGMCC: Chinese General Microbiological Culture Collection Center, Beijing, China; COAD: Culture Collection of Octávio de Almeida Drumond. Universidade Federal de Viçosa, Viçosa, Brasil; FAU: Isolates in culture collection of Systematic Mycology and Microbiology Laboratory; ICMP: International Collection of Micro-organisms from Plants, Auckland, New Zealand; KUMCC: Kumming Institute of Botany, Kumming, China; LGMF, Laboratório de Genética de Microrganismos (LabGeM) culture collection, at the Federal University of Paraná, Brazil; MAFF: Ministry of Agriculture, Forestry and Fisheries, Tokyo, Japan; MFLUCC: Mae Fah Luang University Culture Collection, Chiang Rai, Thailand; SAUCC: Shandong Agricultural University Culture Collection, Shandong, China; STE-U: Department of Plant Pathology, Stellenbosch University, Stellenbosch, South Africa; URM: Culture Collection at the Universidade Federal de Pernambuco, Recife, Brazil; VTCC: Vietnam Type Culture Collection, Center of Biotechnology, Vietnam National University, Hanoi, Vietnam; ZH-KUCC: Culture Collection of Zhongkai University of Agriculture and Engineering, Guangzhou, China. [T] indicates type material.

[2]ITS: internal transcribed spacers and intervening 5.8S nrDNA; *tub2*: partial β-tubulin gene; *his3*: partial histone H3 gene; *tef1*: partial elongation factor 1-alpha gene; *cal*: partial calmodulin gene.

Small-scale fermentation and extraction

The fungus was cultivated in three different liquid media (YM 6.3 medium: 10g/mL malt extract, 4g/mL, yeast extract, 4g/mL, D-glucose and pH = 6.3, Q6 ½ medium: 10 g/mL glycerin, 2.5 g/mL D-glucose, 5 g/mL cotton seed flour and pH = 7.2; ZM ½ medium: 5 g/mL molasses, 5 g/mL oatmeal, 1.5 g/mL D-glucose, 4 g/mL saccharose, 4 g/mL mannitol, 0.5 g/mL edamin, ammonium sulphate 0.5 g/mL, 1.5 g/mL calcium carbonate and pH = 7.2) (Chepkirui et al. 2016). A well-grown 14-day-old mycelial culture grown on YM agar was cut into small pieces using a cork borer (7mm), and five pieces used for inoculation of 500 mL Erlenmeyer flasks containing 200 mL of media. The cultures were incubated at 23 °C on a rotary shaker at 140 rpm. The growth of the fungus was monitored by checking the amount of free glucose daily using Medi-Test glucose strips (Macherey Nagel, Düren, Germany). The fermentation was terminated three days after glucose depletion and the biomasses and supernatants were separated via vacuum filtration. Afterwards, the supernatants were extracted with equal amount of ethyl acetate (200 mL) and filtered through anhydrous sodium sulphate. The resulting ethyl acetate extracts were evaporated to dryness *in vacuo* (Rotary Evaporator: Heidolph Instruments GmbH & Co. KG, Schwabach, Germany; pump: Vacuubrand GmbH & Co. KG, Wertheim am Main, Germany) at 40 °C. The mycelia were extracted with 200 mL of acetone in an ultrasonic bath (Sonorex Digital 10 P, Bandelin Electronic GmH & Co. KG, Berlin, Germany) at 40 °C for 30 min, filtered and the organic phase evaporated. The volume of the remaining aqueous phase was adjusted with an equal amount of distilled water and subjected to the same procedure as described for the supernatants.

The small-scale cultivation of *Diaporthe breyniae* was also carried out on YM agar medium and rice solid medium (BRFT, brown rice 28 g as well as 0.1 L of base liquid (yeast extract 1 g/L, di-sodium tartrate di-hydrate 0.5 g/L, KH_2PO_4 0.5 g/L) (Becker et al. 2020a). Briefly, the fungus was grown on a YM agar plate and the mycelia was extracted with 200 mL of ethyl acetate in an ultrasonic water bath at 40 °C for 30 min, filtered and the filtrate evaporated to dryness *in vacuo* at 40 °C. For BFRT medium, three small pieces of the mycelial culture grown on a YM agar plate were inoculated into a 250 ml Erlenmeyer flask containing 100 mL of YM 6.3 medium. The seed culture was incubated at 23 °C under shake condition at 140 rpm. After 5 days, 10 mL of this seed culture were transferred to a 500 mL Erlenmeyer flask containing BRFT medium and incubated for 28 days at 23 °C. Afterwards, extraction of the culture was performed following the same procedure as above mentioned for the mycelia obtained from the liquid cultures.

Scale-up fermentation in shake flask batches and extraction

Preliminary results obtained from small-scale screening suggested that the fungus grew and produced best in ZM ½ medium (Suppl. material 1: Figs S1, S2). Moreover, the extracts obtained from the fungal culture in ZM ½ were active against *Bacillus subtilis*

and *Mucor plumbeus*. Therefore, this medium was selected for scale-up fermentation. Three well-grown 14-day-old YM agar plate of the mycelial culture were cut into small pieces using a 7 mm cork borer and 5 pieces inoculated in 10 × 500 mL Erlenmeyer flasks containing 200 mL of ZM ½ medium. The culture was incubated at 23 °C on a rotary shaker at 140 rpm for 11 days. Fermentation was aborted 3 days after the depletion of free glucose. The mycelia and supernatant from the batch fermentation were separated *via* vacuum filtration. The mycelia were extracted with 3 × 500 mL of acetone in an ultrasonic water bath at 40 °C for 30 min. The extracts were combined and the solvent evaporated *in vacuo* (40 °C). The remaining water phase was subjected to the same procedure as previously described for the mycelial fraction in small-scale extraction, repeating the extraction step 3 times, yielding 955 mg dark brown solid-like extract. The supernatant (2 L) was extracted with equal amount of ethyl acetate and filtered through anhydrous sodium sulphate. The resulting ethyl acetate extract was evaporated to dryness *in vacuo* to afford 251 mg of extract.

Isolation of secondary metabolites

The mycelial and the supernatant extracts from shake flask batch fermentation dissolved in methanol were centrifuged by means of a centrifuge (Hettich Rotofix 32 A, Tuttlingen, Germany) for 10 min at 4000 rpm. Afterwards, the mycelia and supernatant extracts were fractionated separately using preparative reverse phase HPLC (Büchi, Pure C-850, 2020, Switzerland). VP Nucleodur 100-5 C18ec column (150 × 40 mm, 7 μm: Machery-Nagel, Düren, Germany) was used as stationary phase. Deionized water (Milli-Q, Millipore, Schwalbach, Germany) supplemented with 0.1% formic acid (FA) (solvent A) and acetonitrile (ACN) with 0.1% FA (solvent B) were used as the mobile phase. The elution gradient used for fractionation was 5–35% solvent B for 20 min, 35–80% B for 30 min, 80–100% B for 10 min and thereafter isocratic condition at 100% solvent B for 15 min. The flow rate was set to 30 mL/min and UV detection was carried out at 210, 320 and 350 nm. For the supernatant extract, 13 fractions (F1-F13) were selected according to the observed peaks, and further analysis of the fractions using HPLC-MS revealed that four of the obtained fractions constituted pure compounds. Using the same elution conditions as mentioned, the mycelia extract afforded 17 fractions (F1–F17) selected from the observed peaks. HPLC-MS analysis of the obtained fractions revealed that seven fractions constituted pure compounds. The compounds obtained from mycelial and supernatant extracts were combined according to their respective HPLC-ESIMS retention time and molecular weight. Compound **1** (55.2 mg, t_R = 7.80 min) was obtained from both the mycelium and supernatant extracts as well as compounds **2** (10.9 mg, t_R = 6.27 min), **3** (2.6 mg, t_R = 11.42 min) and **4** (5.6 mg, t_R = 9.49 min). Compounds **5** (3.6 mg, t_R = 13.46 min), **11** (0.7 mg, t_R = 12.11 min) and **12** (2.0 mg, t_R = 3.83 min) were only isolated from the mycelial extract. Fractions F4 from both the mycelium and supernatant extracts were combined and purified using an Agilent Technologies 1200 Infinity Series semi-

preparative HPLC instrument (Waldbronn, Germany). The elution gradient used was 20–30% solvent B for 5 min followed by isocratic condition at 30% B for 25 min and thereafter increased gradient from 30–100% B for 5 min. VP Nucleodur 100-5 C18ec column (250 × 10 mm, 5 μm: Machery-Nagel, Düren, Germany) was used as stationary phase and the flow rate was 3 mL/min. These fractions afforded compound **13** (2.34 mg, t_R = 5.13 min). Fractions F13 and F14 from the mycelial extract were combined with F12 from the supernatant as they contained the same compounds. The pooled fractions were purified by preparative reverse phase HPLC (Büchi, Pure C-850, 2020, Switzerland). VP Nucleodur 100-5 C18ec column (250 × 21 mm, 5 μm: Machery-Nagel, Düren, Germany) was used as stationary phase with a flow rate of 15 mL/min and an elution gradient of 5–70% solvent B for 5 min, followed by isocratic conditions at 70% B for 25min, and thereafter increased gradient from 70–100% B for 5 min. These fractions afforded compound **9** (10.5 mg, t_R = 13.02 min) and sub-fraction G1. Sub-fraction G1 was further purified using an Agilent Technologies 1200 Infinity Series semi-preparative HPLC with the elution gradient starting from 65–70% B for 5 min followed by isocratic condition at 70% B for 25 min and thereafter increased gradient from 70–100% B for 5 min to afford compounds **7** (1.4 mg, t_R = 13.91 min) and **8** (0.52 mg, t_R = 13.56 min). Fraction F15 from the mycelium were also purified using the same instrument and same elution conditions as described for sub-fraction G1. This fraction afforded compounds **6** (1.1 mg, t_R = 14.02 min) and **10** (1.7 mg, t_R = 13.58 min).

Note: The given retention times were obtained from HPLC-ESIMS following the HPLC parameters as described in the general experimental procedures.

Antimicrobial assay

The antifungal and antibacterial activities (Minimum Inhibition Concentration, MIC) of all extracts obtained from small-scale fermentation were determined in serial dilution assays as described previously (Chepkirui et al. 2016; Becker et al. 2020b) against *Bacillus subtilis*, *Candida tenuis*, *Escherichia coli* and *Mucor plumbeus*. The assays were carried out in 96-well microtiter plates in YM 6.3 medium for filamentous fungi and yeast and MHB medium (Müller-Hinton Broth: SN X927.1, Carl Roth GmbH, Karlsruhe, Germany) for bacteria. Starting concentration for all extracts were 300 μg/mL. In addition, the antimicrobial activity of the isolated pure compounds was also assessed as previously described (Matio Kemkuignou et al. 2020) against a panel of bacteria and fungi including *Pichia anomala* DSM 6766, *Schizosaccharomyces pombe* DSM 70572, *Mucor hiemalis* DSM 2656, *Candida albicans* DSM 1665, and *Rhodotorula glutinis* DSM 10134 for fungal microorganisms, *Bacillus subtilis* DSM 10, *Staphyloccocus aureus* DSM 346 and *Mycobacterium smegmatis* ATCC 700084 for Gram-positive bacteria, *Acinetobacter baumannii* DSM 30008, *Chromobacterium violaceum* DSM 30191, *Escherichia coli* DSM 1116 and *Pseudomonas aeruginosa* for Gram-negative bacteria. Starting concentration for tested compounds was adjusted to 66.7 μg/mL.

Cytotoxicity assay

The *in vitro* cytotoxicity (IC_{50}) of the isolated metabolites against several mammalian cell lines (human endocervical adenocarcinoma KB 3.1, mouse fibroblasts L929, squamous cancer A431, breast cancer MCF-7, lung cancer A549, ovary cancer SK-OV-3 and prostate cancer PC-3) was determined by colorimetric tetrazolium dye MTT assay using epothilone B as a positive control in accordance to our previously reported experimental procedure (Becker et al. 2020b).

Results and discussion

Phylogenetic study

The lengths of the fragments of the first phylogenetic inference using the five previously mentioned loci used in the combined dataset for the tree including all *Diaporthe* spp. were 454 bp (ITS), 318 bp (*cal*), 296 bp (*his3*), 153 bp (*tef1*) and 487 bp (*tub2*), comprising in total 341 taxa. The length of the final alignment was 1708 bp. The inferred phylogeny with the best maximum likelihood score with bootstrap support (bs) values mapped onto branch bipartitions is shown in Suppl. material 1: Fig. S100. The here studied strain was located in a clade with 92% bs including 341 taxa, including species belonging to the *D. sojae* complex. A second molecular phylogeny was inferred including sequences of the same loci, but restricted to the aforementioned clade, including 98 taxa. The lengths of the fragments used in the combined dataset were 572 bp (ITS), 449 bp (*cal*), 373 bp (*his3*), 452 bp (*tef1*) and 862 bp (*tub2*), totaling 2708 bp for the final alignment. Fig. 1 shows the consensus ML tree, including bs and Bayesian posterior probability (pp) values at the nodes. Our strain was located in an independent branch distant from other species of *Diaporthe*, demonstrating that this represented a new species, which is introduced here as *D. breyniae*. Unfortunately, the new species lacked sporulation in all media tested in the present study. Therefore, the introduction of it is based only on molecular data.

Taxonomy

Diaporthe breyniae Y. Marín & C. Lamb., sp. nov.
MycoBank No: 843243

Etymology. Name refers to the host genus that this fungus was isolated from, *Breynia*.
   Description. Not sporulated. *Diaporthe breyniae* differs from its closest phylogenetic neighbour, *D. durionigena* by unique fixed alleles in three loci based on alignments of the separate loci included in the supplementary material: ITS positions 93 (indel), 159 (G), 436 (T), 437 (C), 451 (G), 453 (A), 485 (C); *tef1* positions 46 (A), 62 (G), 80 (T), 100 (G), 146 (T), 274 (indel), 304 (A), 310 (G), 313 (C), 339 (T), 343 (A), 385 (G); *tub2* positions 393 (A), 402 (indel), 426 (A), 565 (C), 675 (T), 713 (G), 770 (T).

Figure 1. ML (lnL = -28100.2019) phylogram obtained from the combined ITS, *cal*, *his3*, *tef1* and *tub2* sequences of our strain and related *Diaporthe* spp. *Diaporthe amygdali* CBS 126679[T] and *D. eres* CBS 138594[T] were used as an outgroup. Bootstrap support values ≥ 70/Bayesian posterior probability scores ≥ 0.95 are indicated along branches. Branch lengths are proportional to distance. New taxon is indicated in bold. Type material of the different species is indicated with [T].

Culture characters. Colonies on PDA reaching 55–70 mm in 2 weeks, greyed yellow (161A) with a white ring and transparent margins, lobate, cottony, raised, margins filamentous to fimbriate; reverse greyed yellow (161A–D) with transparent margins. Colonies on MEA covering the surface of the Petri dish in 2 weeks, white with greyed yellow center (161A), velvety to cottony, flat to raised in some zones, margins filamentous to fimbriate; reverse greyed yellow (162A–B). Colonies on OA covering the surface of the Petri dish in 2 weeks, white with greyed yellow ring (161D), velvety, flat, margins filamentous to fimbriate; reverse grey brown (199D).

Specimen examined. CAMEROON, Kala mountain, on leaves of *Breynia oblongifolia*, 02 Jan. 2019, *S.C.N. Wouamba* (holotype: CBS H-24920, culture ex-type CBS 148910 = STMA 18284).

Notes. *Diaporthe breyniae* is introduced based only on molecular data since sporulation could not be induced in any media used. This species is located in a well-supported clade (97% bs / 1 pp) together with *D. durionigena*, *D. passifloricola*, *D. rosae*, *D. thunbergiicola*, *D. ueckeri* and *D. vochysiae*. The latter species has only been reported from Brazil occurring on different hosts, i.e. *Stryphnodendron adstringens* (Fabaceae, Fabales) and *Vochysia divergens* (Vochysiaceae, Myrtales) (Noriler et al. 2019). *Diaporthe durionigena* has been only isolated from *Durio zibethinus* (Malvaceae, Malvales) in Vietnam (Crous et al. 2020, 2021). *Diaporthe passifloricola* has been found on *Passiflora foetida* (Passifloraceae, Malpighiales) and *Citrus* spp. (Rutaceae, Sapindales) in China and Malaysia (Crous et al. 2016; Chaisiri et al. 2021; Dong et al. 2021), while *D. rosae* has been isolated from *Rosa* sp. (Rosaceae, Rosales), *Magnolia champaca* (Magnoliaceae, Magnoliales) and *Senna siamea* (Fabaceae, Fabales) in Thailand (Perera et al. 2018; Wanasinghe et al. 2018). *Diaporthe ueckeri* (syn. *D. miriciae*, Gao et al. 2016) has been reported in Australia, Colombia and the USA, on *Cucumis melo* (Cucurbitaceae, Cucurbitales), *Glycine max* (Fabaceae, Fabales) and *Helianthus annuus* (Asteraceae, Asterales) (Thompson et al. 2015; Udayanga et al. 2015; López-Cardona et al. 2021). *Diaporthe thunbergiicola* has been only isolated from *Thunbergia laurifolia* (Acanthaceae, Lamiales) in Thailand (Liu et al. 2015). The new species *D. breyniae* is the only of these species reported on *Breynia* (Phyllanthaceae, Malpighiales) in Africa. In fact, to the best of our knowledge, this is the first species of *Diaporthe* reported in Cameroon and occurring in this host.

Structure elucidation of compounds 1–13

Cultivation trials carried out on *Diaporthe breyniae* in different culture media including YM 6.3, Q6 ½, ZM ½, rice solid and YM agar highlighted its potential for producing secondary metabolites. During antimicrobial screening of the extracts, the fungus revealed significant antifungal and antibacterial activity against *Mucor hiemalis* and *Bacillus subtilis* respectively, especially when cultured in ZM ½ medium, encouraging more detailed examination. Investigation into the chemistry of *Diaporthe breyniae* led to the isolation of two new secondary metabolites (**7**, **8**) together with eleven known compounds (**1–4**, **5**, **6**, **9–13**) from the EtOAc extracts of a 2 L scale-up ZM ½ liquid

medium of the fungus (Fig. 2). The structure elucidation of **1–13** was determined by detailed spectroscopic analysis of their 1D and 2D NMR data in combination with their HR-ESIMS data.

HR-ESI(+)MS and NMR spectroscopic analysis identified compounds **1–3** as cytochalasin H (**1**) (Suppl. material 1: Figs S3–S10) (Beno et al. 1977; Shang et al. 2017), deacetylcytochalasin H or cytochalasin J (**2**) (Suppl. material 1: Figs S11–S17) (Cole et al. 1981; Shang et al. 2017) and cytochalasin RKS-1778 (**3**) (Suppl. material 1: Figs S18–S24) (Kakeya et al. 1997) respectively. The absolute configuration of cytochalasins H (**1**) and J (**2**) was confirmed by comparing their optical rotation values ($[\alpha]^{20}_D$ +55.7 (c 0.158, MeOH) for 1 and $[\alpha]^{20}_D$ +35.3 (c 0.394, MeOH) for **2**) and ECD spectrum (Fig. 3) with those reported in the literature (Shang et al. 2017; Ma et al. 2021). The literature reports only the relative configuration of compound **3** (*rel-* (3*S*, 4*R*, 5*S*, 8*S*, 9*S*, 13*E*, 16*S*, 18*R*, 19*E*, 21*R*)) (Kakeya et al. 1997), therefore, its absolute configuration was investigated by comparison of its ECD spectrum with that of cytochalasins H (**1**) and J (**2**) (Fig. 3). The ECD spectrum of **3** showed negative (~200 nm) cotton effect, the shape of which matched with that of compounds **1** and **2**. Thus, the hitherto unestablished absolute configuration of cytochalasin RKS-1778 (**3**) was confirmed to be 3*S*, 4*R*, 5*S*, 8*R*, 9*R*, 13*E*, 16*S*, 18*R*, 19*E*, 21*R*.

HR-ESI (+) MS analysis of **4** isolated as a yellowish oil afforded pseudo-molecular ion peaks [M+H]+ at *m/z* 436.2852 and [M+Na]+ at *m/z* 458.2665 attributed to the molecular formula $C_{28}H_{37}NO_3$ (11 degrees of unsaturation). Comparison of the 1D and 2D NMR spectroscopic data for 4 (DMSO-d_6) with those for **3** (Table 2) revealed that both compounds are closely related, with compound **4** being the deacetylated derivative of **3**. This was confirmed on the 1H NMR spectrum of compound **4** by the absence of the methyl group H$_3$-25 and on its 13C NMR spectrum by the absence of both C-24 carbonyl group and C-25 methyl group as visible on the NMR data recorded for compound **3** (Table 2). The relative configuration of compound **4** was determined by analysis of the coupling constants and NOESY correlations. The E-geometry of the $\Delta^{13,14}$ and $\Delta^{19,20}$ double bonds in the macrocyclic ring was determined based on the large coupling constants *J* = 15.3 and 16.7 Hz observed between H-13 and H-14 and between H-19 and H-20 respectively. The small coupling constant *J* = 4.4 Hz observed between H-4 and H-5 confirmed their *cis* relationship (Kakeya et al. 1997). The NOESY spectrum arbitrarily suggested *a*-orientation of H-3, H-11, H-21 and H-23 based on the observed correlations between H-3/H-11, H-20/H-21 and H-20/H-23,while the *β*-orientation of H-4, H-5, H-8, H-16, 18-OH and 21-OH were apparent from a network NOESY correlations between H-4/H-5, H-5/H-8, H-8/21-OH, 21-OH/H-19, H-19/H-16 and H-16/18-OH (Fig. 4). These correlations allowed the assignment of the relative configuration of compound **4** as either *rel-* (3*S*, 4*R*, 5*S*, 8*S*, 9*S*, 13*E*, 16*S*, 18*R*, 19*E*, 21*R*) or *rel-* (3*R*, 4*S*, 5*R*, 8*R*, 9*R*, 13*E*, 16*R*, 18*S*, 19*E*, 21*S*). In addition, the optical rotation value of **4** ($[\alpha]^{20}_D$ -17.6 (c 0.278, MeOH)) approximating that reported in the literature for **3** ($[\alpha]^{20}_D$ -20 (c 0.05, MeOH, Kakeya et al. 1997) revealed that both compounds are levorotatory, and this suggested the stereochemistry of **4** to be identical to that of **3**. The latter assumption was confirmed
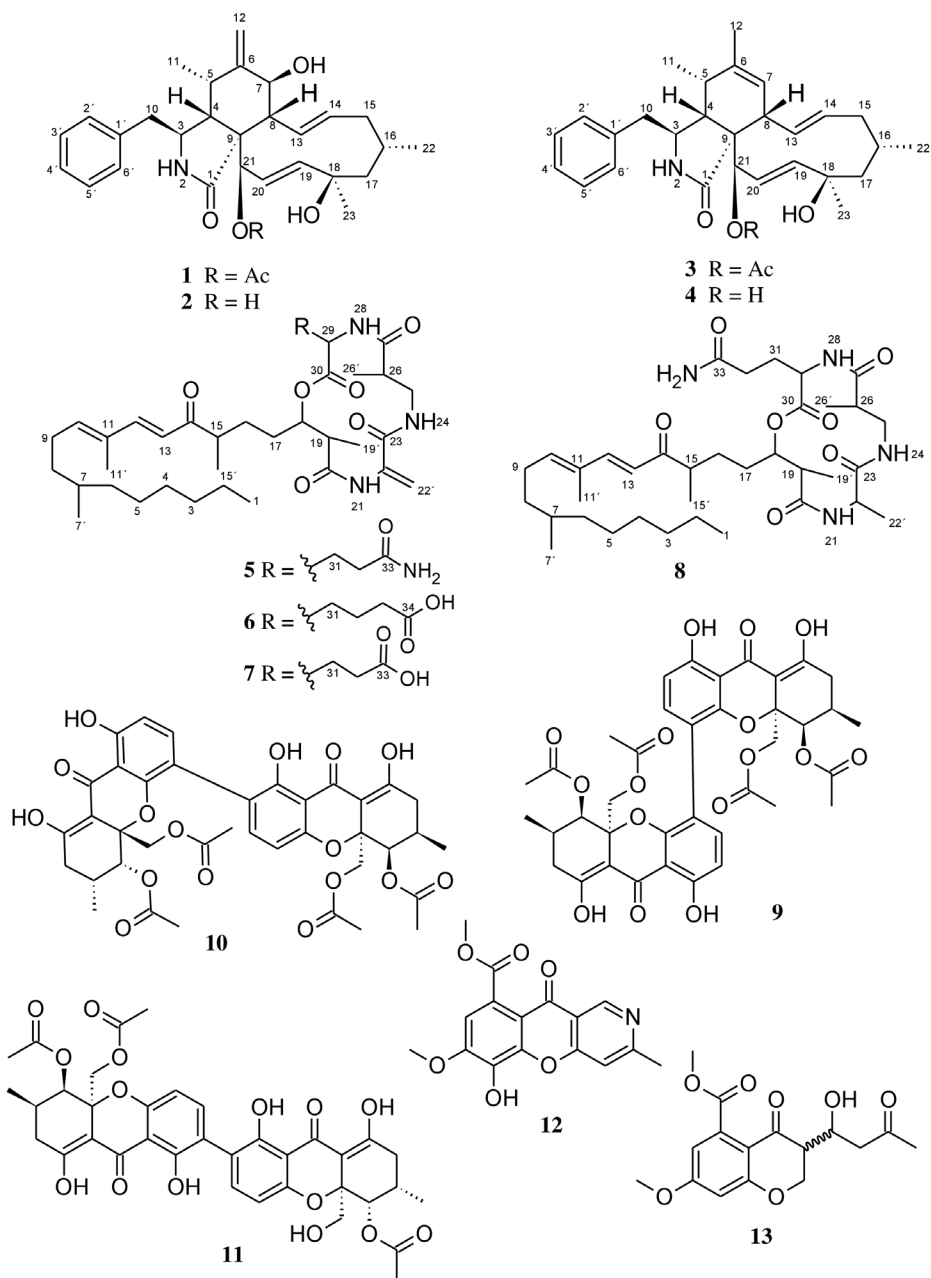
Figure 2. Chemical structures of compounds **1–13** isolated from *Diaporthe breyniae*.

by comparing the ECD spectrum of **4** with those of compounds **1**, **2** and **3**. The same negative Cotton effect (~200 nm) observed for all those compounds unambiguously certified the absolute configuration of compound **4** established as 3*S*, 4*R*, 5*S*, 8*S*, 9*S*,
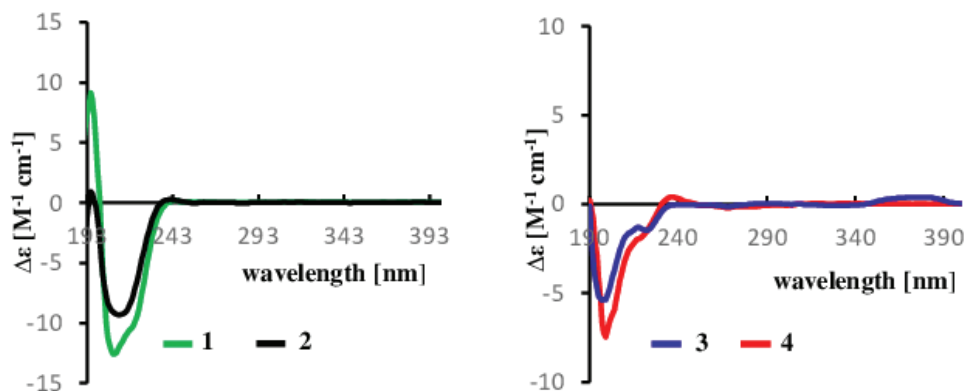
Figure 3. ECD spectra of compounds **1**–**4** in MeOH.

13*E*, 16*S*, 18*R*, 19*E*, 21*R*. Thus, the structure of **4** was determined. This compound was regarded new while the current study has been under review, but concurrently it was published as phomopchalasin N by Chen et al. (2022). Interestingly, the authors also isolated it from a member of the genus *Diaporthe*, but inadvertently referred to their producer organism under the outdated name "*Phomopsis*". We have decided to leave our complete data on the structure elucidation in the manuscript, so they can be compared with those of Chen et al. (2022) by other scientists, but the compounds are indeed identical.

Compounds **5** and **6** were readily identified as the known fusaristatins A and B respectively, after careful analysis of their HR-ESI (+) MS and NMR spectroscopic data (Suppl. material 1: Figs S34–S47). Fusaristatins A (**5**) and B (**6**) were first reported in 2007 from an endophytic *Fusarium* sp. (Shiono et al. 2007) and so far, only fusaristatin A (**5**) has been isolated from *D. phaeseolorum* and *D. longicolla* (syn: *Phomopsis longicolla*) (Santos et al. 2011; Choi et al. 2013; Cui et al. 2017). Therefore, this is the first report for the isolation of fusaristatin B (**6**) from the genus *Diaporthe*. In addition, two new derivatives of fusaristatin A (**7**, **8**) were isolated from *Diaporthe breyniae* and their structures were established by intensive analysis of their 1D and 2D NMR spectroscopic data in combination with HR-ESIMS data and by comparison with the data reported in the literature for fusaristatins A (**5**) and B (**6**) (Shiono et al. 2007).

The molecular formula of compound **7**, isolated as a colorless oil, was determined to be $C_{36}H_{57}N_3O_8$ from the HR-ESIMS (positive mode) which showed pseudo-molecular ion peaks [M+H]⁺ at *m/z* 660.4219 and [M+Na]⁺ at *m/z* 682.4024, indicating 10 degrees of unsaturation. Inspection of the molecular formula of **7** ($C_{36}H_{57}N_3O_8$) in comparison to that of **5** ($C_{36}H_{58}N_4O_7$) suggested that an amino group (-NH₂) in compound **5** could probably have been replaced by a hydroxyl group (-OH) in compound **7**. Intensive analysis of 1D and 2D NMR spectroscopic data (C_5D_5N) of compound **7** in comparison to that of **5** indicated that most signals in **7** were the same as those for **5** (Table 3), implying that **7** and **5** are closely related. The only difference was observed on the ¹H NMR spectrum where the signal corresponding to the amino

Table 2. ^{13}C (125 MHz) and ^{1}H-NMR (500 MHz) spectroscopic data (DMSO-d_6, δ in ppm) of compounds **3**, **4**.

No.	3		4	
	δ_C, type	δ_H (J in Hz)	δ_C, type	δ_H (J in Hz)
1	174.3, C	-	175.9, C	-
2-NH	-	7.89, s	-	7.57, s
3	53.9, CH	3.16, m	53.8, CH	3.14, q (4.9)
4	50.5, CH	2.02, t (4.1)	50.9, CH	2.47, t (4.4)
5	34.1, CH	2.18, m*	34.3, CH	2.3, m
6	137.3, C	-	137.1, C	-
7	126.8, CH	5.21*	127.4, CH	5.17, br s
8	42.3, CH	3.06 br d (9.9)	40.9, CH	3.04, br d (9.8)
9	55.5, C	-	57.2, C	-
10	44.0, CH$_2$	2.59, dd (13.2, 7.4) 2.74, dd (13.1, 5.3)	43.6, CH$_2$	2.65, dd (13.6, 5.2) 2.70, dd (13.6, 5.2)
11	12.8, CH$_3$	0.64, d (7.2)	13.0, CH$_3$	0.84, d (7.3)
12	19.2, CH$_3$	1.62, s	19.3, CH$_3$	1.63, s
13	129.2, CH	5.73, dd (15.7, 10.1)	129.7, CH	5.66, dd (15.3, 10.1)
14	133.5, CH	5.08, ddd (15.3, 10.9, 4.5)	132.8, CH	5.02, ddd (15.3, 11.0, 4.4)
15	42.1, CH$_2$	1.57, m* 1.89, br dd (12.4, 4.3)	42.3, CH$_2$	1.52, q (12.5) 1.84, br dd (12.5, 4.2)
16	27.6, CH	1.69, m	27.7, CH	1.69, m
17	53.1, CH	1.37, br dd (13.6, 3.2) 1.59, m*	53.1, CH$_2$	1.34, br dd (13.4, 3.3) 1.60, dd (13.6, 3.3)
18	72.1, C	-	72.2, C	-
19	137.3, CH	5.36, dd (16.6, 2.3)	136.2, CH	5.61, dd (16.7, 2.4)
20	125.1, CH	5.71, dd (16.9, 2.4)	130.7, CH	5.76, dd (16.7, 2.4)
21	75.7, CH	5.23*	73.7, CH	3.63, br s
22	25.8, CH$_3$	0.94, d (7.3)	25.9, CH$_3$	0.93, d (7.1)
23	31.0, CH$_3$	1.13, s	31.5, CH$_3$	1.12, s
24	169.3, C	-	-	-
25	20.2, CH$_3$	2.18, s	-	-
1′	136.8, C	-	136.9, C	-
2′/6′	129.6, CH (x2)	7.12, d (7.0)	129.8, CH (x2)	7.21*
3′/5′	127.9, CH (x2)	7.29, t (7.5)	127.7, CH (x2)	7.29, t (7.7)
4′	126.0, CH	7.21, t (7.5)	126.0, CH	7.21*
18-OH	-	4.36, s	-	4.17, s
21-OH	-	-	-	4.88, br d (5.6)

*overlapping signals, assignments were supported by HSQC and HMBC

group 34-NH$_2$ (δ_H 8.34) in compound **5** was absent in compound **7** (Table 3). Moreover, in the HMBC spectrum of **7**, correlations from H-31 to C-30, H-31/H-32 to C-33 suggested the presence of a glutamic acid residue instead of a glutamine residue as observed in **5**. Based on ^{1}H-^{1}H COSY, ^{1}H-^{13}C HSQC and ^{1}H-^{13}C HMBC experiments (Fig. 5), the signals of all protons and carbons in the molecule were unambiguously assigned and compound **7** was identified as a new derivative of fusaristatin A named fusaristatin G.

Compound **8** was obtained as a white amorphous solid. The molecular formula was established as $C_{36}H_{60}N_4O_7$ on the basis of the pseudo-molecular ion peaks [M+H]$^+$ at m/z 661.4542 and [M+Na]$^+$ at m/z 683.4354 observed in the HR-ESI(+)MS, indicating 9 double bond equivalents. The molecular formula of **8** ($C_{36}H_{60}N_4O_7$) compared to that of **5** ($C_{36}H_{58}N_4O_7$) showed an increase of 2 Da suggesting that a reduction occurred in compound **5** to afford compound **8**. This assumption was confirmed on
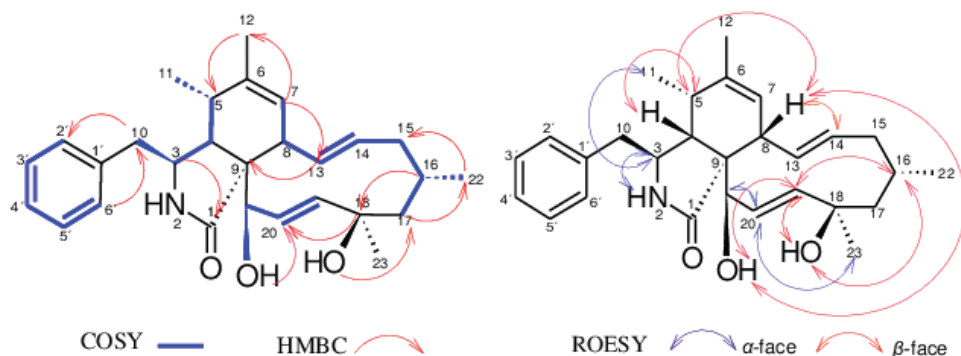
Figure 4. Selected ¹H–¹H COSY, NOESY and HMBC correlations of 4.

the ¹H NMR spectrum of **8** where the signals in the downfield region corresponding to H_a-22′ (δ_H 5.60) and H_b-22′ (δ_H 6.24) as observed in **5** were missing, but instead the signal in the upfield region corresponding to a methyl group H_3-22′ at δ_H 1.65 was recorded (Table 3). Moreover, an additional signal observed on the ¹H NMR of **8** attributable to the methine H-22 (δ_H 4.89) further confirmed this assumption, indicating that the reduction of **5** occurred on the $\Delta^{22\text{-}22'}$ double bond to afford **8**. The reduction of the double bond $\Delta^{22\text{-}22'}$ further justified the upfield shift of the nitrogen-bearing proton 21-NH, which resonated at δ_H 8.15 in compound 8 instead of δ_H 10.43 as in compound 5. In the HMBC spectrum, the correlations observed between H-22′ and C-22/C-23, H-22 and C-22′/C-23 confirmed the presence of an alanine residue instead of dehydroalanine residue as previously reported for **5** (Shiono et al. 2007). Finally, the unambiguous assignment of all proton and carbon signals in metabolite **8** was achieved based on ¹H-¹³C HSQC and ¹H-¹³C HMBC experiments, thus identifying compound **8** as a new derivative of fusaristatin A, for which the trivial name fusaristatin H was assigned.

Compounds **9**–**13** were respectively identified as phomoxanthones A (**9**) and B (**10**) (Isaka et al. 2001), dicerandrol B (**11**) (Wagenaar and Clardy 2001), phomochromenone C (**12**) (Ding et al. 2017; Wei et al. 2021), and diaporchromanone C (**13**) (Wei et al. 2021) by comparison of their HR-ESIMS and 1D and 2 D NMR spectroscopic data (Suppl. material 1: Figs S65–S99) with those reported in the literature.

Physico-chemical characteristic of compounds 4, 7 and 8

Phomopchalasin N (**4**): Yellowish oil. $[\alpha]^{20}_D$ -17.6 (c 0.278, MeOH), UV (MeOH, c = 0.013 mg/mL) λ_{max} (log ɛ) 202 (4.32) nm. CD (c = 2.83 × 10⁻³ M, MeOH) λ_{max} (Δɛ) 200 (-7.66) nm. HR-ESIMS *m/z* 458.2665 [M + Na]⁺, *m/z* 893.5440 [2M + Na]⁺, *m/z* 871.5621 [2M + H]⁺, *m/z* 418.2746 [M + H - H_2O]⁺, *m/z* 436.2852 [M + H]⁺ (Calcd for $C_{28}H_{38}NO_3^+$ 436.2846), t_R = 10.47 min. For NMR data (¹H: 500 MHz, ¹³C: 125 MHz, DMSO-d_6), see Table 2.

Fusaristatin G (**7**): colorless oil. $[\alpha]^{20}_{D}$ -8 (*c* 0.1, MeOH), UV (MeOH, c = 0.02 mg/mL) λ_{max} (log ε) 201 (4.21), 283 (3.96) nm. HR-ESIMS *m/z* 682.4024 [M + Na]⁺, *m/z* 1341.8157 [2M + Na]⁺, *m/z* 1319.8354 [2M + H]⁺, *m/z* 642.4102 [M + H

Table 3. ¹³C and ¹H-NMR spectroscopic data (pyridine-d_5, δ in ppm) of compounds **5**, **7**, **8**.

No.	δ_C, type (5[a])	δ_H (J in Hz) (5[a])	δ_C, type (7[b])	δ_H (J in Hz) (7[b])	δ_C, type (8[b])	δ_H (J in Hz) (8[b])
1	14.7, CH₃	0.88*	14.7, CH₃	0.87*	14.5, CH₃	0.87, t (6.9)*
2	23.4, CH₂	1.20~1.31, m*	23.4, CH₂	1.20~1.31, m*	23.1, CH₂	1.20~1.31, m*
3	32.6, CH₂	1.20~1.31, m*	32.6, CH₂	1.20~1.31, m*	32.3, CH₂	1.20~1.31, m*
4	27.7, CH₂	1.20~1.31, m*	27.7, CH₂	1.20~1.31, m*	27.4, CH₂	1.20~1.31, m*
5	30.3, CH₂	1.20~1.31, m*	30.3, CH₂	1.20~1.31, m*	30.1, CH₂	1.20~1.31, m*
6	37.5, CH₂	1.09, m* 1.20-1.31, m*	37.5, CH₂	1.09, m* 1.20~1.31, m*	37.3, CH₂	1.09, m* 1.20~1.31, m*
7	33.2, CH	1.39, m*	33.2, CH	1.40, m*	32.9, CH	1.38, m*
7′	20.0, CH₃	0.88*	20.0, CH₃	0.88*	19.8, CH₃	0.87, d (6.9)*
8	36.8, CH₂	1.20~1.31* 1.40, m*	36.9, CH₂	1.20~1.31, m* 1.40, m*	36.6, CH₂	1.20~1.31, m* 1.40, m*
9	27.2, CH₂	2.19, m*	27.2, CH₂	2.18, m	27.0, CH₂	2.21, m*
10	144.5, CH	6.03, br t (7.4)	144.5, CH	6.03, br t (7.2)	144.3, CH	6.01, t (7.4)
11	133.9, C	-	140.0, C	-	133.9, C	-
11′	12.6, CH₃	1.83, s	12.7, CH₃	1.83, s	12.5, CH₃	1.85, s
12	148.4, CH	7.54, d (15.7)	148.3, CH	7.56, d (15.7)	148.2, CH	7.55, d (15.7)
13	123.7, CH	6.40, d (15.7)	123.8, CH	6.40, d (15.7)	123.6, CH	6.45, d (15.7)
14	203.8, C	-	203.6, C	-	204.1, C	-
15	44.5, CH	2.84, m	44.6, CH	2.80~2.88, m*	44.6, CH	2.88, m
15′	17.7, CH₃	1.10, d (6.9)	17.6, CH₃	1.10, d (6.9)	17.1, CH₃	1.13, d (6.9)
16	28.5, CH₂	1.57, m 1.93~2.00, m*	28.3, CH₂	1.54, m 1.93~2.00, m*	29.1, CH₂	1.66, m 2.04, m*
17	30.3, CH₂	1.87, m 1.93~2.00, m*	30.2, CH₂	1.84, m 1.93~2.00, m*	31.3, CH₂	1.97, m 2.04, m*
18	77.3, CH	5.44, m	77.2, CH	5.48, m	77.6, CH	5.45, m
19	44.6, CH	3.03, quin (7.0)	44.5, CH	3.05, quin (7,0)	45.6, CH	2.95, m
19′	15.8, CH₃	1.30, d (7.0)*	15.9, CH₃	1.33, d (7.3)*	14.9, CH₃	1.35, d (7.3)
20	173.9, C	-	174.0, C	-	173.5, C	-
21-NH	-	10.43, s	-	10.55, s	-	8.15, br s
22	139.6, C	-	139.8, C	-	50.9, CH	4.89, m
22′	114.6, CH₂	5.60, s 6.24, s	114.3, CH₂	5.59, s 6.22, s	17.3, CH₃	1.65, d (7.1)
23	165.2, C	-	165.3, C	-	173.9, C	-
24-NH	-	7.81, br s	-	7.88, br t (6.1)	-	7.96, br s
25	43.0, CH₂	3.81, dt (13.5, 6.9) 3.92, dt (13.3, 4.9)	43.0, CH₂	3.78, dt (13.5, 6.7) 3.94, m	42.1, CH₂	3.49, dt (13.6, 3.8) 4.04, dt (13.5, 7.9)
26	42.7, CH	2.87, m	42.7, CH	2.92, m	42.8, CH	2.85, m
26′	15.5, CH₃	1.30, d (7.0)*	15.8, CH₃	1.33, d (7.3)*	14.9, CH₃	1.22, d (7.3)
27	175.0, C	-	175.1, C	-	175.4, C	-
28-NH	-	9.06, br d (7.5)	-	9.11, br d (7.7)	-	8.90, br d (7.7)
29	53.6, CH	5.13, dd (14.3, 7.6)	53.4, CH	5.18, m*	53.6, CH	5.06, dd (12.9, 6.2)
30	172.3, C	-	172.4, C	-	172.5, C	-
31	27.6, CH₂	2.63, dt (13.7, 7.0) 2.69~2.77, m*	27.5, CH₂	2.62, dt (13.8, 6.9) 2.71, tt (13.8, 6.9)	27.3, CH₂	2.51, m 2.68~2.74, m*
32	32.8, CH₂	2.69~2.77, m*	32.1, CH₂	2.80~2.88, m*	32.7, CH₂	2.68~2.74, m*
33	175.7, C	-	176.1, C	-	176.7, C	-
34-NH₂	-	8.34, s	-	-	-	8.32, br s

*overlapping signals: assignments were supported by HSQC and HMBC, [a]¹H 500 MHz, ¹³C 125 MHz; [b]¹H 700 MHz, ¹³C 175 MHz.
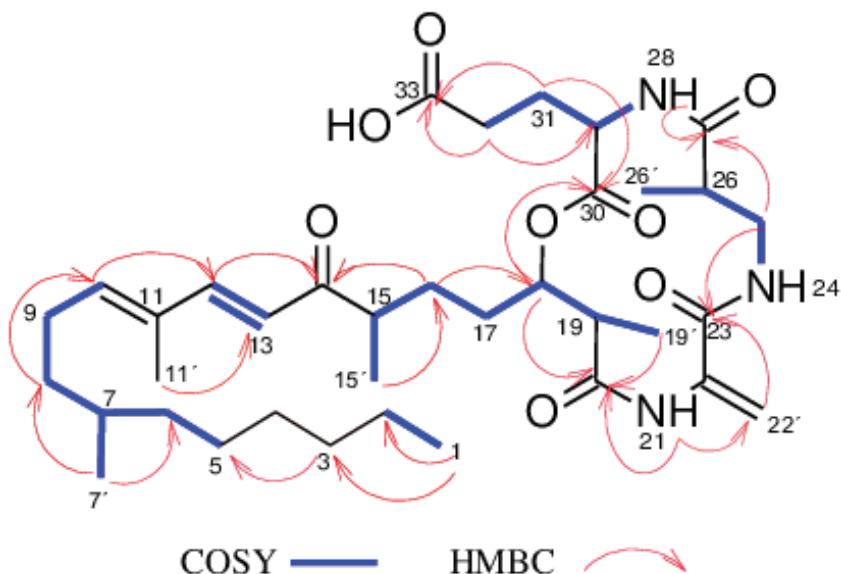
Figure 5. Selected ^{1}H–^{1}H COSY and HMBC correlations of **7**.

- H$_2$O]$^+$, *m/z* 660.4219 [M + H]$^+$ (Calcd for C$_{36}$H$_{58}$N$_3$O$_8$$^+$ 660.4218), t_R = 14.80 min. For NMR data (^{1}H: 700 MHz, ^{13}C: 175 MHz, C$_5$H$_5$N-d_5), see Table 3.

Fusaristatin H (**8**): White amorphous solid. [α]$^{20}_D$ +14 (*c* 0.03, MeOH), UV (MeOH, c = 0.02 mg/mL) λ$_{max}$ (log ε) 201 (4.24), 283 (4.20) nm. HR-ESIMS *m/z* 683.4354 [M + Na]$^+$, *m/z* 1343.8820 [2M + Na]$^+$, *m/z* 1321.9000 [2M + H]$^+$, *m/z* 661.4542 [M + H]$^+$ (Calcd for C$_{36}$H$_{61}$N$_4$O$_7$$^+$ 661.4535), t_R = 14.46 min. For NMR data (^{1}H: 700 MHz, ^{13}C: 175 MHz, C$_5$H$_5$N-d_5), see Table 3.

Biological activity

The extracts obtained from the fungal culture in ZM ½ exhibited activities against *Bacillus subtilis* with MIC values of 75 μg/mL for the supernatant´s extract and 2.3 μg/mL for the mycelial extract. These extracts were also active against *Mucor plumbeus* with respective MIC values of 150 and 37.5 μg/mL. Moreover, the purified compounds **1–7**, **9**, **10**, **12**, and **13** were subjected to antimicrobial assays against a panel of bacteria and fungi. The minimum inhibitory concentration (MIC) values showed that all compounds were active against at least one of the tested micro-organisms at concentration of 66.7 μg/mL (Table 4). Overall, the majority of the tested compounds exhibited weak to moderate activity. However, significant activity was noted for phomoxanthones A (**9**) and B (**10**) against *Bacillus subtilis*. Both compounds inhibited the growth of the latter bacterium with a MIC value of 1.7 μg/mL, which turned out to be 5 times stronger than that of oxytetracyclin used as positive control. In addition, their MIC value of 4.2 μg/mL against the Gram-positive bacterium *S. aureus* was

quite considerable in comparison to that of the other tested compounds. This finding concurs well with previously published data which reported the antimicrobial activity of xanthone derivatives isolated from *Diaporthe* spp. (Wagenaar and Clardy 2001; Elsässer et al. 2005; Lim et al. 2010). The antimicrobial activity of dicerandrol B (**11**), a closely related congener of phomoxanthones A (**9**) and B (**10**) was not investigated in the present work due to the low amount of available sample, however, its activity against *B. subtilis* and *S. aureus* has previously been reported (Wagenaar and Clardy 2001). The antimicrobial activity of compound 8 was not assessed due to the paucity of the sample.

The cytotoxicity of all the isolated compounds except **11** was evaluated against a panel of mammalian cell lines. Eight compounds, **1–5** and **8–10** showed activity in this assay whereas the other isolated metabolites were inactive under test conditions (Table 5). The very significant activity exhibited by compounds **1–4** against all tested cancer cell lines were in agreement with previous studies which have reported cytochalasins as potent cytotoxins (Shang et al. 2017). However, when comparing the activity of the cytochalasin **4**, which is the deacetylated derivative of **3**, it was quite interesting to notice that **4** is significantly less toxic than **3** leading to the hypothesis that the presence of the acetyl group in **3** is an important structural element in the biological activity of the studied cytochalasins. The aforementioned assumption, was also observed when comparing the cytotoxicity of compound **1** and **2**. In effect, **2** is the deacetylated derivative of **1**, and the latter was also found to be less toxic than **1**. These results therefore give some hints in regards to the structure activity relationship (SAR) of the isolated cytochalasins, which will be tested further for their inhibitory effect on actin. In the same assay, compound **5** and **8** were found to be active against KB3.1 cell line with IC_{50} value of 10.63 and 30.3 µM respectively whereas compound **6** and **7** bearing the same core skeleton did not show any activity. These results indicated that the cytotoxicity of this class of compounds might possibly be enhanced by the presence of an amide group (C-33) as

Table 4. Minimum Inhibitory Concentrations (MIC) of compounds **1–7**, **9–10**, **12–13** against tested microorganisms.

| Test organisms | MIC (µg/mL) | | | | | | | | | | | References |
	1	2	3	4	5	6	7	9	10	12	13	
Acinetobacter baumanii	-	-	-	-	-		-	-	-	-	-	0.26[c]
Bacillus subtilis	-	-	16.7	66.7	16.7		16.7	1.7	1.7	66.7		8.3[o]
Candida albicans	-	-	-	-	-	-		66.7	-	-	-	16.6[n]
Chromobacterium violaceum	-	-	-	-	-	-	-	-	-	-	-	0.83[o]
Escherichia coli	-	-	-	-	-	-	-	-	-	-		1.7[o]
Mucor hiemalis	66.7	-	66.7	66.7	66.7	66.7	66.7	16.7	66.7	66.7	66.7	8.3[n]
Mycobacterium smegmatis	-	-	-	-	-	-	-	66.7	-	-	-	1.7[k]
Pichia anomala	-	-	-	-	-	-	-	-	-	-	-	8.3[n]
Pseudomonas aeruginosa	-	-	-	-	-	-	-	-	-	-	-	0.21[g]
Rhodoturula glutinis	66.7	-	-	-	-	-	-	-	-	-	-	4.2[n]
Schizosaccharomyces pombe	16.7	66.7	66.7	66.7	-	-	-	-	66.7	-	-	8.3[n]
Staphylococcus aureus	-	-	66.7	66.7	66.7		66.7	4.2	4.2	66.7	-	0.83[o]

(-): No inhibition, [c]Ciprobay 2.54 mg/mL, [g]Gentamycin 1 mg/mL, [k]Kanamycin 1 mg/mL, [n]Nystatin 1 mg/mL, [o]Oxytetracyclin 1 mg/mL. Starting concentration for antimicrobial assay were 66.7 µg/mL.

Table 5. Cytotoxic activity of compounds **1–10**, **12–13**.

Cell lines	1	2	3	4	5	6	7	8	9	10	12	13	Epothilone B
					IC$_{50}$ (µM)								
KB3.1	0.064	0.33	1.7	5.8	10.6	-	-	30.3	0.36	0.91	-	-	$6.5×10^{-5}$
L929	0.19	1.5	1.3	10.8	>30.4	-	-	-	1.06	5.6	-	-	$6.5×10^{-4}$
A431	0.085	0.33	14.3	11.0	12.0	n.t	n.t	n.t	0.04	0.17	n.t	n.t	$1.2×10^{-4}$
MCF-7	0.14	3.1	7.3	19.3	7.44	n.t	n.t	n.t	0.02	0.36	n.t	n.t	$8.2×10^{-5}$
A549	0.16	0.73	3.1	10.3	19.7	n.t	n.t	n.t	0.43	1.0	n.t	n.t	$6.1×10^{-5}$
SKOV-3	0.073	0.33	13.6	45.9	13.9	n.t	n.t	n.t	0.15	0.65	n.t	n.t	$2.9×10^{-4}$
PC-3	0.14	0.29	4.2	9.4	7.3	n.t	n.t	n.t	1.1	9.7	n.t	n.t	$9.5×10^{-4}$

n.t: not tested, (-): no activity. Starting concentration for cytotoxicity assay was 37 µg/mL

shown in **5** and **8** instead of a carboxylic acid as observed in **6** (C-34) and 7 (C-33). In addition, phomoxanthones A (**9**) and B (**10**), exhibited strong cytotoxic activities with half-maximal inhibitory concentrations (IC$_{50}$) in the range 0.02 – 9.7 µM. These results were in accordance with previous published cytotoxicity of dimeric tetrahydroxanthone derivatives against human epidermoid carcinoma (KB), human breast cancer (BC-1), mouse lymphoma (L5178Y), human ovarian carcinoma (A2780), and African monkey kidney fibroblast (Vero) cell lines among others (Isaka et al. 2001; Rönsberg et al. 2013).

Conclusion

The genus *Diaporthe* has been regarded for decades as a potential source for the production of diverse bioactive secondary metabolites. In the present study, we suggest the introduction of the new species *D. breyniae* isolated from the twigs of *Breynia oblongifolia* in Cameroon. From the liquid culture of this fungus, two previously undescribed polyketides were isolated together with eleven known compounds. The isolated compounds showed weak to strong antimicrobial activities as well as moderate cytotoxic activities overall. These results demonstrated that it should certainly be worthwhile to explore untapped geographic area like the African tropics in general and Cameroon in particular for the discovery of new fungi and the isolation of novel secondary metabolites produced by these with significant biological activities.

Acknowledgments

References

Alfaro ME, Zoller S, Lutzoni F (2003) Bayes or bootstrap. A simulation study comparing the performance of Bayesian Markov chain Monte Carlo sampling and bootstrapping in assessing phylogenetic confidence. Molecular Biology and Evolution 20(2): 255–266. https://doi.org/10.1093/molbev/msg028

Becker K, Wongkanoun S, Wessel AC, Bills GF, Stadler M, Luangsa-Ard JJ (2020a) Phylogenetic and chemotaxonomic studies confirm the affinities of *Stromatoneurospora phoenix* to the coprophilous Xylariaceae. Journal of Fungi (Basel, Switzerland) 6(3): 1–21. https://doi.org/10.3390/jof6030144

Becker K, Wessel AC, Luangsa-Ard JJ, Stadler M (2020b) Viridistratins A–C, antimicrobial and cytotoxic benzo[*j*]fluoranthenes from stromata of *Annulohypoxylon viridistratum* (Hypoxylaceae, Ascomycota). Biomolecules 10(5): 805. https://doi.org/10.3390/biom10050805

Beno MA, Christoph GG, Cox RH, Wells JM, Cole RJ, Kirksey JW (1977) Structure of a New [1 l]Cytochalasin, Cytochalasin H or Kodo-cytochalasin-1. Journal of the American Chemical Society 99(12): 4123–4130. https://doi.org/10.1021/ja00454a035

Carbone I, Kohn LM (1999) A method for designing primer sets for the speciation studies in filamentous ascomycetes. Mycologia 91(3): 553–556. https://doi.org/10.1080/00275514.1999.12061051

Chaisiri C, Liu X-Y, Yin W-X, Luo C-X, Lin Y (2021) Morphology characterization, molecular phylogeny, and pathogenicity of *Diaporthe passifloricola* on *Citrus reticulata* cv. Nanfengmi-ju in Jiangxi Province, China. Plants 10(2): e218. https://doi.org/10.3390/plants10020218

Chang CQ, Cheng YH, Xiang MM, Jiang ZD (2005) New species of *Phomopsis* on woody plants in Fujian Province. Junwu Xuebao 24: 6–11.

Chen Y, Yang W, Zou G, Wang G, Kang W, Yuan J, She Z (2022) Cytotoxic bromine- and iodine-containing cytochalasins produced by the mangrove endophytic fungus *Phomopsis* sp. QYM-13 using the OSMAC approach. Journal of Natural Products. https://doi.org/10.1021/acs.jnatprod.1c01115

Chepkirui C, Stadler M (2017) The genus *Diaporthe*: A rich source of diverse and bioactive metabolites. Mycological Progress 16(5): 477–494. https://doi.org/10.1007/s11557-017-1288-y

Chepkirui C, Richter C, Matasyoh JC, Stadler M (2016) Monochlorinated calocerins A-D and 9-oxostrobilurin derivatives from the basidiomycete *Favolaschia calocera*. Phytochemistry 132: 95–101. https://doi.org/10.1016/j.phytochem.2016.10.001

Chernomor O, von Haeseler A, Monh BQ (2016) Terrace aware data structure for Phylogenomic Inference from Supermatrices. Systematic Biology 65(6):997-1008. https://doi.org/10.1093/sysbio/syw037

Choi JN, Kim J, Ponnusamy K, Lim C, Kim JG, Muthaiya MJ, Lee CH (2013) Metabolic Changes of *Phomopsis longicolla* Fermentation and Its Effect on Antimicrobial Activity Against *Xanthomonas oryzae*. Journal of Microbiology and Biotechnology 23(2): 177–183. https://doi.org/10.4014/jmb.1210.10020

Cole RJ, Wells JM, Cox RH, Cutler HG (1981) Isolation and biological properties of deacetylcytochalasin H from *Phomopsis* sp. Journal of Agricultural and Food Chemistry 29(1): 205–206. https://doi.org/10.1021/jf00103a057

Crous PW, Groenewald JZ, Risede JM, Simoneau P, Hyde KD (2004) *Calonectria* species and their *Cylindrocladium* anamorphs: Species with sphaeropedunculate vesicles. Studies in Mycology 50: 415–430. https://doi.org/10.3114/sim.55.1.213

Crous PW, Summerell BA, Shivas RG, Romberg M, Mel'nik VA, Verkley GJM, Groenewald JZ (2011) Fungal Planet description sheets: 92–106. Persoonia 27(1): 130–162. https://doi.org/10.3767/003158511X617561

Crous PW, Wingfield MJ, Schumacher RK, Summerell BA, Giraldo A, Gené J, Guarro J, Wanasinghe DN, Hyde KD, Camporesi E, Garethjones EB, Thambugala KM, Malysheva EF, Malysheva VF, Acharya K, Álvarez J, Alvarado P, Assefa A, Barnes CW, Bartlett JS, Blanchette RA, Burgess TI, Carlavilla JR, Coetzee MPA, Damm U, Decock CA, Denbreeÿen A, Devries B, Dutta AK, Holdom DG, Rooney-Latham S, Manjón JL, Marincowitz S, Mirabolfathy M, Moreno G, Nakashima C, Papizadeh M, Shahzadehfazeli SA, Amoozegar MA, Romberg MK, Shivas RG, Stalpers JA, Stielow B, Stukely MJC, Swart WJ, Tan YP, Vanderbank M, Wood AR, Zhang Y, Groenewald JZ (2014) Fungal Planet description sheets: 281–319. Persoonia 33(1): 212–289. https://doi.org/10.3767/003158514X685680

Crous PW, Wingfield MJ, Le Roux JJ, Richardson DM, Strasberg D, Shivas RG, Alvarado P, Edwards J, Moreno G, Sharma R, Sonawane MS, Tan YP, Altés A, Barasubiye T, Barnes CW, Blanchette RA, Boertmann D, Bogo A, Carlavilla JR, Cheewangkoon R, Daniel R, de Beer ZW, Yáñez-Morales M de Jesús, Duong TA, Fernández-Vicente J, Geering ADW, Guest DI, Held BW, Heykoop M, Hubka V, Ismail AM, Kajale SC, Khemmuk W, Kolařík M, Kurli R, Lebeuf R, Lévesque CA, Lombard L, Magista D, Manjón JL, Marincowitz S, Mohedano JM, Nováková A, Oberlies NH, Otto EC, Paguigan ND, Pascoe IG, Pérez-Butrón JL, Perrone G, Rahi P, Raja HA, Rintoul T, Sanhueza RMV, Scarlett K, Shouche YS, Shuttleworth LA, Taylor PWJ, Thorn RG, Vawdrey LL, Solano-Vidal R, Voitk A, Wong PTW, Wood AR, Zamora JC, Groenewald JZ (2015) Fungal Planet description sheets: 371–399. Persoonia 35(1): 264–327. https://doi.org/10.3767/003158515X690269

Crous PW, Wingfield MJ, Richardson DM, Leroux JJ, Strasberg D, Edwards J, Roets F, Hubka V, Taylor PWJ, Heykoop M, Martín MP, Moreno G, Sutton DA, Wiederhold NP, Barnes CW, Carlavilla JR, Gené J, Giraldo A, Guarnaccia V, Guarro J, Hernández-Restrepo M, Kolařík M, Manjón JL, Pascoe IG, Popov ES, Sandoval-Denis M, Woudenberg JHC, Acharya K, Alexandrova AV, Alvarado P, Barbosa RN, Baseia IG, Blanchette RA, Boekhout T, Burgess TI, Cano-Lira JF, Čmoková A, Dimitrov RA, Dyakov MY, Dueñas M, Dutta AK, Esteve-Raventós F, Fedosova AG, Fournier J, Gamboa P, Gouliamova DE, Grebenc T, Groenewald M, Hanse B, Hardy GESTJ, Held BW, Jurjević Ž, Kaewgrajang T, Latha KPD, Lombard L, Luangsaard JJ, Lysková P, Mallátová N, Manimohan P, Miller AN, Mirabolfathy M, Morozova OV, Obodai M, Oliveira NT, Ordóñez ME, Otto EC, Paloi S, Peterson SW, Phosri C, Roux J, Salazar WA, Sánchez A, Sarria GA, Shin H-D, Silva BDB, Silva GA, Smith MTH, Souza-

Motta CM, Stchigel AM, Stoilova-Disheva MM, Sulzbacher MA, Telleria MT, Toapanta C, Traba JM, Valenzuela-Lopez N, Watling R, Groenewald JZ (2016) Fungal Planet description sheets: 400–468. Persoonia 36(1): 316–458. https://doi.org/10.3767/003158516X692185

Crous PW, Carnegie AJ, Wingfield MJ, Sharma R, Mughini G, Noordeloos ME, Santini A, Shouche YS, Bezerra JDP, Dima B, Guarnaccia V, Imrefi I, Jurjević Ž, Knapp DG, Kovács GM, Magistà D, Perrone G, Rämä T, Rebriev YA, Shivas RG, Singh SM, Souza-Motta CM, Thangavel R, Adhapure NN, Alexandrova AV, Alfenas AC, Alfenas RF, Alvarado P, Alves AL, Andrade DA, Andrade JP, Barbosa RN, Barili A, Barnes CW, Baseia IG, Bellanger J-M, Berlanas C, Bessette AE, Bessette AR, Biketova AYu, Bomfim FS, Brandrud TE, Bransgrove K, Brito ACQ, Cano-Lira JF, Cantillo T, Cavalcanti AD, Cheewangkoon R, Chikowski RS, Conforto C, Cordeiro TRL, Craine JD, Cruz R, Damm U, de Oliveira RJV, de Souza JT, de Souza HG, Dearnaley JDW, Dimitrov RA, Dovana F, Erhard A, Esteve-Raventós F, Félix CR, Ferisin G, Fernandes RA, Ferreira RJ, Ferro LO, Figueiredo CN, Frank JL, Freire KTLS, García D, Gené J, Gęsiorska A, Gibertoni TB, Gondra RAG, Gouliamova DE, Gramaje D, Guard F, Gusmão LFP, Haitook S, Hirooka Y, Houbraken J, Hubka V, Inamdar A, Iturriaga T, Iturrieta-González I, Jadan M, Jiang N, Justo A, Kachalkin AV, Kapitonov VI, Karadelev M, Karakehian J, Kasuya T, Kautmanová I, Kruse J, Kušan I, Kuznetsova TA, Landell MF, Larsson K-H, Lee HB, Lima DX, Lira CRS, Machado AR, Madrid H, Magalhães OMC, Majerova H, Malysheva EF, Mapperson RR, Marbach PAS, Martín MP, Martín-Sanz A, Matočec N, McTaggart AR, Mello JF, Melo RFR, Mešič A, Michereff SJ, Miller AN, Minoshima A, Molinero-Ruiz L, Morozova OV, Mosoh D, Nabe M, Naik R, Nara K, Nascimento SS, Neves RP, Olariaga I, Oliveira RL, Oliveira TGL, Ono T, Ordoñez ME, de M Ottoni A, Paiva LM, Pancorbo F, Pant B, Pawłowska J, Peterson SW, Raudabaugh DB, Rodríguez-Andrade E, Rubio E, Rusevska K, Santiago ALCMA, Santos ACS, Santos C, Sazanova NA, Shah S, Sharma J, Silva BDB, Siquier JL, Sonawane MS, Stchigel AM, Svetasheva T, Tamakeaw N, Telleria MT, Tiago PV, Tian CM, Tkalčec Z, Tomashevskaya MA, Truong HH, Vecherskii MV, Visagie CM, Vizzini A, Yilmaz N, Zmitrovich IV, Zvyagina EA, Boekhout T, Kehlet T, Læssøe T, Groenewald JZ (2019) Fungal Planet description sheets: 868–950. Persoonia 42: 291–473. https://doi.org/10.3767/persoonia.2019.42.11

Crous PW, Wingfield MJ, Chooi Y-H, Gilchrist CLM, Lacey E, Pitt JI, Roets F, Swart WJ, Cano-Lira JF, Valenzuela-Lopez N, Hubka V, Shivas RG, Stchigel AM, Holdom DG, Jurjević Ž, Kachalkin AV, Lebel T, Lock C, Martín MP, Tan YP, Tomashevskaya MA, Vitelli JS, Baseia IG, Bhatt VK, Brandrud TE, De Souza JT, Dima B, Lacey HJ, Lombard L, Johnston PR, Morte A, Papp V, Rodríguez A, Rodríguez-Andrade E, Semwal KC, Tegart L, Abad ZG, Akulov A, Alvarado P, Alves A, Andrade JP, Arenas F, Asenjo C, Ballarà J, Barrett MD, Berná LM, Berraf-Tebbal A, Bianchinotti MV, Bransgrove K, Burgess TI, Carmo FS, Chávez R, Čmoková A, Dearnaley JDW, Santiago ALCMA, Freitas-Neto JF, Denman S, Douglas B, Dovana F, Eichmeier A, Esteve-Raventós F, Farid A, Fedosova AG, Ferisin G, Ferreira RJ, Ferrer A, Figueiredo CN, Figueiredo YF, Reinoso-Fuentealba CG, Garrido-Benavent I, Cañete-Gibas CF, Gil-Durán C, Glushakova AM, Gonçalves MFM, González M, Gorczak M, Gorton C, Guard FE, Guarnizo AL, Guarro J, Gutiérrez M, Hamal P, Hien LT, Hocking AD, Houbraken J, Hunter GC, Inácio CA, Jourdan M, Kapitonov VI, Kelly L, Khanh TN, Kisło K, Kiss L, Kiyashko A, Kolařík M, Kruse J, Kubátová A, Kučera V, Kučerová I, Kušan I, Lee HB, Levicán G, Lewis A, Liem NV, Liimatainen K, Lim HJ, Lyons MN, Maciá-Vicente JG, Magaña-Dueñas V, Mahiques R, Malysheva EF, Marbach

PAS, Marinho P, Matočec N, McTaggart AR, Mešić A, Morin L, Muñoz-Mohedano JM, Navarro-Ródenas A, Nicolli CP, Oliveira RL, Otsing E, Ovrebo CL, Pankratov TA, Paños A, Paz-Conde A, Pérez-Sierra A, Phosri C, Pintos Á, Pošta A, Prencipe S, Rubio E, Saitta A, Sales LS, Sanhueza L, Shuttleworth LA, Smith J, Smith ME, Spadaro D, Spetik M, Sochor M, Sochorová Z, Sousa JO, Suwannasai N, Tedersoo L, Thanh HM, Thao LD, Tkalčec Z, Vaghefi N, Venzhik AS, Verbeken A, Vizzini A, Voyron S, Wainhouse M, Whalley AJS, Wrzosek M, Zapata M, Zeil-Rolfe I, Groenewald JZ (2020) Fungal Planet description sheets: 1042–1111. Persoonia 44(1): 301–459. https://doi.org/10.3767/persoonia.2020.44.11

Crous PW, Hernández-Restrepo M, Schumacher RK, Cowan DA, Maggs-Kölling G, Marais E, Wingfield MJ, Yilmaz N, Adan OCG, Akulov A, Duarte E Álvarez, Berraf-Tebbal A, Bulgakov TS, Carnegie AJ, de Beer ZW, Decock C, Dijksterhuis J, Duong TA, Eichmeier A, Hien LT, Houbraken JAMP, Khanh TN, Liem NV, Lombard L, Lutzoni FM, Miadlikowska JM, Nel WJ, Pascoe IG, Roets F, Roux J, Samson RA, Shen M, Spetik M, Thangavel R, Thanh HM, Thao LD, van Nieuwenhuijzen EJ, Zhang JQ, Zhang Y, Zhao LL, Groenewald JZ (2021) New and Interesting Fungi. 4. Fungal Systematics and Evolution 7: 255–343. https://doi.org/10.3114/fuse.2021.07.13

Cui H, Yu J, Chen S, Ding M, Huang X, Yuan J, She Z (2017) Alkaloids from the mangrove endophytic fungus *Diaporthe phaseolorum* SKS019. Bioorganic & Medicinal Chemistry Letters 27(4): 803–807. https://doi.org/10.1016/j.bmcl.2017.01.029

da Silva RMF, Soares AM, Pádua APSL, Firmino AL, Souza-Motta CM, da Silva GA, Plautz Jr HL, Bezerra JDP, Paiva LM, Ryvarden L, Oliani LC, de Mélo MAC, Magalhães OMC, Pereira OL, Oliveira RJV, Oliveira TGS, Svedese VM, Fan XL (2019) Mycological Diversity Description II. Acta Botanica Brasílica 33(1): 163–173. https://doi.org/10.1590/0102-33062018abb0411

de Silva NI, Maharachchikumbura SSN, Thambugala KM, Bhat DJ, Karunarathna SC, Tennakoon DS, Phookamsak R, Jayawardena RS, Lumyong S, Hyde KD (2021) Morphomolecular taxonomic studies reveal a high number of endophytic fungi from *Magnolia candolli* and *M. garrettii* in China and Thailand. Mycosphere: Journal of Fungal Biology 11(1): 163–237. https://doi.org/10.5943/mycosphere/12/1/3

Ding B, Wang Z, Xia G, Huang X, Xu F, Chen W, She Z (2017) Three new chromone derivatives produced by *Phomopsis* sp. HNY29-2B from *Acanthus ilicifolius* Linn. Wiley Online Library 35(12): 1889–1893. https://doi.org/10.1002/cjoc.201700375

Dissanayake AJ, Camporesi E, Hyde KD, Zhang W, Yan JY, Li XH (2017) Molecular phylogenetic analysis reveals seven new *Diaporthe* species from Italy. Mycosphere: Journal of Fungal Biology 8(5): 853–877. https://doi.org/10.5943/mycosphere/8/5/4

Dissanayake AJ, Chen Y-Y, Liu J-K (2020) Unravelling *Diaporthe* species associated with woody hosts from karst formations (Guizhou) in China. Journal of Fungi 6: e251. https://doi.org/10.3390/jof6040251

Doilom M, Dissanayake AJ, Wanasinghe DN, Boonmee S, Liu J-K, Bhat DJ, Taylor JE, Bahkali AH, McKenzie EHC, Hyde KD (2017) Microfungi on *Tectona grandis* (teak) in Northern Thailand. Fungal Diversity 82: 107–182.

Dong Z, Manawasinghe IS, Huang Y, Shu Y, Phillips AJL, Dissanayake AJ, Hyde KD, Xiang M, Luo M (2021) Endophytic *Diaporthe* associated with *Citrus grandis* cv. *tomentosa* in China. Frontiers in Microbiology 11: e3621. https://doi.org/10.3389/fmicb.2020.609387

Elsässer B, Krohn K, Flörke U, Root N, Aust HJ, Draeger S, Schulz B, Antus S, Kurtán T (2005) X-ray structure determination, absolute configuration and biological activity of Phomoxanthone A. European Journal of Organic Chemistry 2005(21): 4563–4570. https://doi.org/10.1002/ejoc.200500265

Feng X-X, Chen J-J, Wang G-R, Cao T-T, Zheng Y-L, Zhang C-L (2019) *Diaporthe sinensis*, a new fungus from *Amaranthus* sp. in China. Phytotaxa 425(5): 259–268. https://doi.org/10.11646/phytotaxa.425.5.1

Gao Y, Liu F, Cai L (2016) Unravelling *Diaporthe* species associated with *Camellia*. Systematics and Biodiversity 14(1): 102–117. https://doi.org/10.1080/14772000.2015.1101027

Gao YH, Liu F, Duan W, Crous PW, Cai L (2017) *Diaporthe* is paraphyletic. IMA Fungus 8(1): 153–187. https://doi.org/10.5598/imafungus.2017.08.01.11

Glass NL, Donaldson GC (1995) Development of primer sets designed for use with the PCR to amplify conserved genes from filamentous ascomycetes. Applied and Environmental Microbiology 61(4): 1323–1330. https://doi.org/10.1128/aem.61.4.1323-1330.1995

Gomes RR, Glienke C, Videira SIR, Lombard L, Groenewald JZ, Crous PW (2013) *Diaporthe*: A genus of endophytic, saprobic and plant pathogenic fungi. Persoonia 31(1): 1–41. https://doi.org/10.3767/003158513X666844

Guarnaccia V, Crous PW (2017) Emerging citrus diseases in Europe caused by *Diaporthe* spp. IMA Fungus 8(2): 317–334. https://doi.org/10.5598/imafungus.2017.08.02.07

Guarnaccia V, Groenewald JZ, Woodhall J, Armengol J, Cinelli T, Eichmeier A, Ezra D, Fontaine F, Gramaje D, Gutierrez-Aguirregabiria A, Kaliterna J, Kiss L, Larignon P, Luque J, Mugnai L, Naor V, Raposo R, Sándor E, Váczy KZ, Crous PW (2018) *Diaporthe* diversity and pathogenicity revealed from a broad survey of grapevine diseases in Europe. Persoonia 40(1): 135–153. https://doi.org/10.3767/persoonia.2018.40.06

Hilário S, Amaral IA, Gonçalves MFM, Lopes A, Santos L, Alves A (2020) *Diaporthe* species associated with twig blight and dieback of *Vaccinium corymbosum* in Portugal, with description of four new species. Mycologia 112(2): 293–308. https://doi.org/10.1080/00275514.2019.1698926

Huang F, Hou X, Dewdney MM, Fu Y, Chen G, Hyde KD, Li H (2013) *Diaporthe* species occurring on citrus in China. Fungal Diversity 61(1): 237–250. https://doi.org/10.1007/s13225-013-0245-6

Huang F, Udayanga D, Wang X, Hou X, Mei X, Fu Y, Hyde KD, Li H (2015) Endophytic *Diaporthe* associated with Citrus, a phylogenetic reassessment with seven new species from China. Fungal Biology 119(5): 331–347. https://doi.org/10.1016/j.funbio.2015.02.006

Huang S, Xia J, Zhang X, Sun W (2021) Morphological and phylogenetic analyses reveal three new species of *Diaporthe* from Yunnan, China. MycoKeys 78: 49–77. https://doi.org/10.3897/mycokeys.78.60878

Hyde KD, Chaiwan N, Norphanphoun C, Boonmee S, Camporesi E, Chethana KWT, Dayarathne MC, de Silva NI, Dissanayake AJ, Ekanayaka AH, Hongsanan S, Huang SK, Jayasiri SC, Jayawardena RS, Jiang HB, Karunarathna A, Lin CG, Liu JK, Liu NG, Lu YZ, Luo ZL, Maharachchimbura SSN, Manawasinghe IS, Pem D, Perera RH, Phukhamsakda C, Samarakoon MC, Senwanna C, Shang QJ, Tennakoon DS, Thambugala KM, Tibpromma, S, Wanasinghe DN, Xiao YP, Yang J, Zeng XY, Zhang JF, Zhang SN, Bulgakov TS, Bhat DJ, Cheewangkoon R, Goh TK, Jones EBG, Kang JC, Jeewon R, Liu ZY, Lumyong S, Kuo CH,

McKenzie EHC, Wen TC, Yan JY, Zhao Q (2018) Mycosphere notes 169–224. Mycosphere: Journal of Fungal Biology 9(2): 271–430. https://doi.org/10.5943/mycosphere/9/2/8

Hyde KD, Dong Y, Phookamsak R, Jeewon R, Bhat DJ, Jones EBG, Liu N-G, Abeywickrama PD, Mapook A, Wei D, Perera RH, Manawasinghe IS, Pem D, Bundhun D, Karunarathna A, Ekanayaka AH, Bao D-F, Li J, Samarakoon MC, Chaiwan N, Lin C-G, Phutthacharoen K, Zhang S-N, Senanayake IC, Goonasekara ID, Thambugala KM, Phukhamsakda C, Tennakoon DS, Jiang H-B, Yang J, Zeng M, Huanraluek N, Liu J-KJ, Wijesinghe SN, Tian Q, Tibpromma S, Brahmanage RS, Boonmee S, Huang S-K, Thiyagaraja V, Lu Y-Z, Jayawardena RS, Dong W, Yang E-F, Singh SK, Singh SM, Rana S, Lad SS, Anand G, Devadatha B, Niranjan M, Sarma VV, Liimatainen K, Aguirre-Hudson B, Niskanen T, Overall A, Alvarenga RLM, Gibertoni TB, Pfliegler WP, Horváth E, Imre A, Alves AL, da Silva Santos AC, Tiago PV, Bulgakov TS, Wanasinghe DN, Bahkali AH, Doilom M, Elgorban AM, Maharachchikumbura SSN, Rajeshkumar KC, Haelewaters D, Mortimer PE, Zhao Q, Lumyong S, Xu J, Sheng J (2020) Fungal diversity notes 1151–1276: Taxonomic and phylogenetic contributions on genera and species of fungal taxa. Fungal Diversity 100(1): 5–277. https://doi.org/10.1007/s13225-020-00439-5

Iantas J, Savi DC, Schibelbein Rd S, Noriler SA, Assad BM, Dilarri G, Ferreira H, Rohr J, Thorson JS, Shaaban KA, Glienke C (2021) Endophytes of Brazilian medicinal plants with activity against phytopathogens. Frontiers in Microbiology 12: e714750. https://doi.org/10.3389/fmicb.2021.714750

Isaka M, Jaturapat A, Rukseree K, Danwisetkanjana K, Tanticharoen M, Thebtaranonth Y (2001) Phomoxanthones A and B, novel xanthone dimers from the endophytic fungus *Phomopsis* species. Journal of Natural Products 64(8): 1015–1018. https://doi.org/10.1021/np010006h

Jouda JB, Tamokou J de D, Mbazoa CD, Douala-Meli C, Sarkar P, Bag PK, Wandji J (2016) Antibacterial and cytotoxic cytochalasins from the endophytic fungus *Phomopsis* sp. harbored in *Garcinia kola* (Heckel) nut. BMC Complementary and Alternative Medicine 16(1): 1–9. https://doi.org/10.1186/s12906-016-1454-9

Kakeya H, Morishita M, Onozawa C, Usami R, Horikoshi K, Kimura KI, Yoshihama M, Osada H (1997) RKS-1778, a new mammalian cell-cycle inhibitor and a key intermediate of the [11]cytochalasin group. Journal of Natural Products 60(7): 669–672. https://doi.org/10.1021/np970151o

Kalyaanamoorthy S, Minh BQ, Wong TKF, von Haeseler A, Jermiin LS (2017) ModelFinder: Fast model selection for accurate phylogenetic estimates. Nature Methods 14(6): 587–589. https://doi.org/10.1038/nmeth.4285

Katoh K, Standley DM (2013) MAFFT multiple sequence alignment software v. 7: Improvements in performance and usability. Molecular Biology and Evolution 30(4): 772–780. https://doi.org/10.1093/molbev/mst010

Kearse M, Moir R, Wilson A, Stones-Havas S, Cheung M, Sturrock S, Buxton S, Cooper A, Markowitz S, Duran C, Thierer T, Ashton B, Mentjies P, Drummond A (2012) Geneious basic: An integrated and extendable desktop software platform for the organization and analysis of sequence data. Bioinformatics (Oxford, England) 28(12): 1647–1649. https://doi.org/10.1093/bioinformatics/bts199

Kretz R, Wendt L, Wongkanoun S, Luangsa-Ard JJ, Surup F, Helaly SE, Noumeur SR, Stadler M, Stradal TEB (2019) The effect of cytochalasans on the actin cytoskeleton of eukaryotic

cells and preliminary structure-activity relationships. Biomolecules 9(2): e73. https://doi.org/10.3390/biom9020073

Kumar S, Stecher G, Li M, Knyaz C, Tamura K (2018) MEGA X: Molecular evolutionary Genetics analysis across computing platforms. Molecular Biology and Evolution 35(6): 1547–1549. https://doi.org/10.1093/molbev/msy096

Lanfear R, Frandsen PB, Wright AM, Senfeld T, Calcott B (2016) PartitionFinder 2: new methods for selecting partitioned models of evolution for molecular and morphological phylogenetic analyses. Molecular Biology and Evolution 34: 772–773. https://doi.org/10.1093/molbev/msw260

Li WJ, McKenzie EHC, Liu JK, Bhat DJ, Dai D-Q, Camporesi E, Tian Q, Maharachchikumbura SSN, Luo Z-L, Shang Q-J, Zhang J-F, Tangthirasunun N, Karunarathna SC, Xu J-C, Hyde KD (2020) Taxonomy and phylogeny of hyaline-spored coelomycetes. Fungal Diversity 100(1): 279–801. https://doi.org/10.1007/s13225-020-00440-y

Lim C, Kim J, Choi JN, Ponnusamy K, Jeon Y, Kim SU, Kim JG, Lee CH (2010) Identification, fermentation, and bioactivity against *Xanthomonas oryzae* of antimicrobial metabolites isolated from *Phomopsis longicolla* S1B4. Journal of Microbiology and Biotechnology 20: 494–500. https://doi.org/10.4014/JMB.0909.09026

Liu JK, Hyde KD, Jones EBG, Ariyawansa HA, Bhat DJ, Boonmee S, Maharachchikumbura SSN, McKenzie EHC, Phookamsak R, Phukhamsakda C, Shenoy BD, Abdel-Wahab MA, Buyck B, Chen J, Chethana KWT, Singtripop C, Dai DQ, Dai YC, Daranagama DA, Dissanayake AJ, Doilom M, D'souza MJ, Fan XL, Goonasekara ID, Hirayama K, Hongsanan S, Jayasiri SC, Jayawardena RS, Karunarathna SC, Li WJ, Mapook A, Norphanphoun C, Pang KL, Perera RH, Peršoh D, Pinruan U, Senanayake IC, Somrithipol S, Suetrong S, Tanaka K, Thambugala KM, Tian Q, Tibpromma S, Udayanga D, Wijayawardene NN, Wanasinghe D, Wisitrassameewong K, Zeng XY, Abdel-Aziz FA, Adamčík S, Bahkali AH, Boonyuen N, Bulgakov T, Callac P, Chomnunti P, Greiner K, Hashimoto A, Hofstetter V, Kang JC, Lewis D, Li XH, Liu XZ, Liu ZY, Matsumura M, Mortimer PE, Rambold G, Randrianjohany E, Sato G, Sri-Indrasutdhi V, Tian CM, Verbeken A, von Brackel W, Wang Y, Wen TC, Xu JC, Yan JY, Zhao RL, Camporesi E (2015) Fungal diversity notes 1–110: Taxonomic and phylogenetic contributions to fungal species. Fungal Diversity 72(1): 1–197. https://doi.org/10.1007/s13225-015-0324-y

Long X, Ding Y, Deng J (2018) Total synthesis of asperchalasines A, D, E, and H. Angewandte Chemie International Edition 130(43): 14417–14420. https://doi.org/10.1002/ange.201808481

López-Cardona N, Guevara-Castro A, Gañán-Betancur L, Amaya-Gómez CV (2021) First report of *Diaporthe ueckerae* causing stem canker on soybean (*Glycine max*) in Colombia. Disease Note. https://doi.org/10.1094/PDIS-04-21-0718-PDN

Ma K-L, Dong S-H, Li H-Y, Wei W-J, Tu Y-Q, Gao K (2021) Cytochalasins from *Xylaria* sp. CFL5, an endophytic fungus of *Cephalotaxus fortunei*. 11: 87–98. https://doi.org/10.1007/s13659-020-00279-5

Manawasinghe IS, Dissanayake AJ, Li X, Liu M, Wanasinghe DN, Xu J, Zhao W, Zhang W, Zhou Y, Hyde KD, Brooks S, Yan J (2019) High genetic diversity and species complexity of *Diaporthe* associated with grapevine dieback in China. Frontiers in Microbiology 10: e1936. https://doi.org/10.3389/fmicb.2019.01936

Mapook A, Hyde KD, McKenzie EHC, Jones EBG, Bhat DJ, Jeewon R, Stadler M, Samarakoon MC, Malaithong M, Tanunchai B, Buscot F, Wubet T, Purahong W (2020) Taxonomic and phylogenetic contributions to fungi associated with the invasive weed *Chromolaena odorata* (Siam weed). Fungal Diversity 101(1): 1–175. https://doi.org/10.1007/s13225-020-00444-8

Marin-Felix Y, Hernandez-Restrepo M, Wingfield MJ, Akulov A, Carnegie AJ, Cheewangkoon R, Gramaje D, Groenewald JZ, Guarnaccia V, Halleen F, Lombard L, Luangsa-ard J, Marincowitz S, Moslemi A, Mostert L, Quaedvlieg W, Schumacher RK, Spies CFJ, Thangavel R, Taylor PWJ, Wilson AM, Wingfield BD, Wood AR, Crous PW (2019) Genera of phytopathogenic fungi: GOPHY 2. Studies in Mycology 92(1): 47–133. https://doi.org/10.1016/j.simyco.2018.04.002

Matio Kemkuignou B, Treiber L, Zeng H, Schrey H, Schobert R, Stadler M (2020) Macrooxazoles A-D, new 2,5-disubstituted oxazole-4-carboxylic acid derivatives from the plant pathogenic fungus *Phoma macrostoma*. Molecules (Basel, Switzerland) 25(23): 1–18. https://doi.org/10.3390/molecules25235497

Milagres CA, Belisário R, Silva MA, Lisboa DO, Pinho DB, Furtado GQ (2018) A novel species of *Diaporthe* causing leaf spot in *Pachira glabra*. Tropical Plant Pathology 43(5): 460–467. https://doi.org/10.1007/s40858-018-0242-0

Minh BQ, Schmidt HA, Chernomor O, Schrempf D, Woodhams MD, von Haeseler A, Lanfear R (2020) IQ-TREE 2: New models and efficient methods for phylogenetic inference in the genomic era. Molecular Biology and Evolution 6–10(5): 1530–1534. https://doi.org/10.1093/molbev/msaa015

Mostert L, Crous PW, Kang J-C, Phillips AJL (2001) Species of *Phomopsis* and a *Libertella* sp. occurring on grapevines with specific reference to South Africa: Morphological, cultural, molecular and pathological characterization. Mycologia 93(1): 146–167. https://doi.org/10.1080/00275514.2001.12061286

Noriler SA, Savi DC, Ponomareva L, Rodrigues R, Rohr J, Thorson JS, Glienke C, Shaaban KA (2019) Vochysiamides A and B: Two new bioactive carboxamides produced by the new species *Diaporthe vochysiae*. Fitoterapia 138: 104–273. https://doi.org/10.1016/j.fitote.2019.104273

Pereira C, Ferreira B, Aucique-Perez C, Barreto R (2021) *Diaporthe rosiphthora* sp. nov.: Yet another rose dieback fungus. Crop Protection (Guildford, Surrey) 139: e105365. https://doi.org/10.1016/j.cropro.2020.105365

Perera RH, Hyde KD, Peršoh D, Jones EBG, Liu JK, Liu ZY (2018) Additions to wild seed and fruit fungi 1: The sexual morph of *Diaporthe rosae* on *Magnolia champaca* and *Senna siamea* fruits in Thailand. Mycosphere : Journal of Fungal Biology 9(2): 256–270. https://doi.org/10.5943/mycosphere/9/2/7

Petrović K, Riccioni L, Dordević V, Tubic SB, Miladinović J, Ceran M, Rajković D (2018) *Diaporthe pseudolongicolla* - the new pathogen on soybean seed in Serbia. Ratarstvo i Povrtarstvo 55(2): 103–109. https://doi.org/10.5937/ratpov55-18582

Ronquist F, Teslenko M, van der Mark P, Ayres DL, Darling A, Höhna S, Larget B, Liu L, Suchard MA, Huelsenbeck JP (2012) MrBayes 3.2: Efficient Bayesian Phylogenetic Inference and Model Choice Across a Large Model Space. Systematic Biology 61(3): 539–542. https://doi.org/10.1093/sysbio/sys029

Rönsberg D, Debbab A, Mándi A, Vasylyeva V, Böhler P, Stork B, Engelke L, Hamacher A, Sawadogo R, Diederich M, Wray V, Lin W, Kassack MU, Janiak C, Scheu S, Wesselborg S,

Kurtán T, Aly AH, Proksch P (2013) Pro-apoptotic and immunostimulatory tetrahydrox-anthone dimers from the endophytic fungus *Phomopsis longicolla*. The Journal of Organic Chemistry 78(24): 12409–12425. https://doi.org/10.1021/jo402066b

Santos JM, Correia VG, Phillips AJL (2010) Primers for mating-type diagnosis in *Diaporthe* and *Phomopsis*, their use in teleomorph induction in vitro and biological species definition. Fungal Biology 114(2–3): 255–270. https://doi.org/10.1016/j.funbio.2010.01.007

Santos JM, Vrandečić K, Ćosić J, Duvnjak T, Phillips AJL (2011) Resolving the *Diaporthe* species occurring on soybean in Croatia. Persoonia 27(1): 9–19. https://doi.org/10.3767/003158511X603719

Santos L, Phillips AJL, Crous PW (2017) *Diaporthe* species on Rosaceae with descriptions of *D. pyracanthae* sp. nov. and *D. malorum* sp. nov. Mycosphere : Journal of Fungal Biology 8(5): 485–511. https://doi.org/10.5943/mycosphere/8/5/1

Shang Z, Raju R, Salim AA, Khalil ZG, Capon RJ (2017) Cytochalasins from an Australian Marine Sediment-Derived *Phomopsis* sp. (CMB-M0042F): Acid-Mediated Intramolecular Cycloadditions Enhance Chemical Diversity. The Journal of Organic Chemistry 82(18): 9704–9709. https://doi.org/10.1021/acs.joc.7b01793

Shiono Y, Tsuchinari M, Shimanuki K, Miyajima T, Murayama T, Koseki T, Laatsch H, Funakoshi T, Takanami K, Suzuki K (2007) Fusaristatins A and B, two new cyclic lipopeptides from an endophytic *Fusarium* sp. The Journal of Antibiotics 60(5): 309–316. https://doi.org/10.1038/ja.2007.39

Smith H, Wingfield MJ, Crous PW, Coutinho TA (1996) *Sphaeropsis sapinea* and *Botryosphaeria dothidea* endophytic in *Pinus* spp. and *Eucalyptus* spp. in South Africa. South African Journal of Botany 62(2): 86–88. https://doi.org/10.1016/S0254-6299(15)30596-2

Stone KJ, Bacon WC, White FJ (2000) An overview of endophytic microbes: endophytism defined. Microbial Endophytes: 17–44. https://doi.org/10.1201/9781482277302-1

Sun W, Huang S, Xia J, Zhang X, Li Z (2021) Morphological and molecular identification of *Diaporthe* species in south-western China, with description of eight new species. MycoKeys 77: 65–95. https://doi.org/10.3897/mycokeys.77.59852

Talavera G, Castresana J (2007) Improvement of phylogenies after removing divergent and ambiguously aligned blocks from protein sequence alignments. Systematic Biology 56(4): 564–577. https://doi.org/10.1080/10635150701472164

Tennakoon DS, Kuo CH, Maharachchikumbura SSN, Thambugala KM, Gentekaki E, Phillips AJL, Bhat DJ, Wanasinghe DN, de Silva NI, Promputtha I, Hyde KD (2021) Taxonomic and phylogenetic contributions to *Celtis formosana*, *Ficus ampelas*, *F. septica*, *Macaranga tanarius* and *Morus australis* leaf litter inhabiting microfungi. Fungal Diversity 108(1): 1–215. https://doi.org/10.1007/s13225-021-00474-w

The Royal Horticultural Society London (1966) R.H.S. Colour Chart. London, UK.

Thompson SM, Tan YP, Young AJ, Neate SM, Aitken EAB, Shivas RG (2011) Stem cankers on sunflower (*Helianthus annuus*) in Australia reveal a complex of pathogenic *Diaporthe* (*Phomopsis*) species. Persoonia 27(1): 80–89. https://doi.org/10.3767/003158511X617110

Thompson SM, Tan YP, Shivas RG, Neate SM, Morin L, Bissett A, Aitken EAB (2015) Green and brown bridges between weeds and crops reveal novel *Diaporthe* species in Australia. Persoonia 35(1): 39–49. https://doi.org/10.3767/003158515X687506

Udayanga D, Liu XZ, Mckenzie EHC, Chukeatirote E, Hyde KD (2012) Multi-locus phylogeny reveals three new species of *Diaporthe* from Thailand. Cryptogamie. Mycologie 33(3): 295–309. https://doi.org/10.7872/crym.v33.iss3.2012.295

Udayanga D, Castlebury LA, Rossman AY, Chukeatirote E, Hyde KD (2014) Insights into the genus *Diaporthe*: Phylogenetic species delimitation in the *D. eres* species complex. Fungal Diversity 67(1): 203–229. https://doi.org/10.1007/s13225-014-0297-2

Udayanga D, Castlebury LA, Rossman AY, Chukeatirote E, Hyde KD (2015) The *Diaporthe sojae* species complex, phylogenetic re-assessment of pathogens associated with soybean, cucurbits and other field crops. Fungal Biology 119(5): 383–407. https://doi.org/10.1016/j.funbio.2014.10.009

Van Rensburg JCJ, Lamprecht SC, Groenewald JZ, Castlebury LA, Crous PW (2006) Characterization of *Phomopsis* spp. associated with die-back of rooibos (*Aspalathus linearis*) in South Africa. Studies in Mycology 55: 65–74. https://doi.org/10.3114/sim.55.1.65

Wagenaar MM, Clardy J (2001) Dicerandrols, new antibiotic and cytotoxic dimers produced by the fungus *Phomopsis longicolla* isolated from an endangered mint. Journal of Natural Products 64(8): 1006–1009. https://doi.org/10.1021/np010020u

Wanasinghe DN, Phukhamsakda C, Hyde KD, Jeewon R, Lee HB, Gareth Jones EB, Tibpromma S, Tennakoon DS, Dissanayake AJ, Jayasiri SC, Gafforov Y, Camporesi E, Bulgakov TS, Ekanayake AH, Perera RH, Samarakoon MC, Goonasekara ID, Mapook A, Li W-J, Senanayake IC, Li J, Norphanphoun C, Doilom M, Bahkali AH, Xu J, Mortimer PE, Tibell L, Tibell S, Karunarathna SC (2018) Fungal diversity notes 709–839: Taxonomic and phylogenetic contributions to fungal taxa with an emphasis on fungi on Rosaceae. Fungal Diversity 89(1): 1–236. https://doi.org/10.1007/s13225-018-0395-7

Wei C, Sun C, Feng Z, Zhang X, Xu J (2021) Four new chromones from the endophytic fungus *Phomopsis asparagi* DHS-48 isolated from the chinese mangrove plant *Rhizophora mangle*. Marine Drugs 19(6): e348. https://doi.org/10.3390/md19060348

White TJ, Bruns T, Lee S, Taylor J (1990) Amplification and direct sequencing of fungal ribosomal genes for phylogenetics. In: Gelfand M, Sninsky JI, White TJ (Eds) PCR protocols: a guide to methods and applications. Academic Press, New York, 315–322. https://doi.org/10.1016/B978-0-12-372180-8.50042-1

Xu TC, Lu YH, Wang JF, Song ZQ, Hou YG, Liu SS, Liu CS, Wu SH (2021) Bioactive secondary metabolites of the genus *diaporthe* and anamorph *phomopsis* from terrestrial and marine habitats and endophytes: 2010–2019. Microorganisms 9(2): 1–49. https://doi.org/10.3390/microorganisms9020217

Yahara I, Harada F, Sekita S, Yoshihira K, Natori S (1982) Correlation between effects of 24 different cytochalasins on cellular structures and cellular events and those on actin in vitro. The Journal of Cell Biology 92(1): 69–78. https://doi.org/10.1083/jcb.92.1.69

Yang Q, Fan X-L, Guarnaccia V, Tian C-M (2018) High diversity of *Diaporthe* species associated with dieback diseases in China, with twelve new species described. MycoKeys 39: 97–149. https://doi.org/10.3897/mycokeys.39.26914

Yuyama KT, Wendt L, Surup F, Kretz R, Chepkirui C, Wittstein K, Boonlarppradab C, Wongkanoun S, Luangsa-ard J, Stadler M, Abraham W-R (2018) Cytochalasans act as inhibitors of biofilm formation of *Staphylococcus* aureus. Biomolecules 8(4): e129. https://doi.org/10.3390/biom8040129

Zaghouani M, Kunz C, Guédon L, Blanchard F, Nay B (2016) First total synthesis, structure revision, and natural history of the smallest cytochalasin: (+)-periconiasin G. Chemistry (Weinheim an der Bergstrasse, Germany) 22(43): 15257–15260. https://doi.org/10.1002/chem.201603734

Zhang D, Gao F, Jakovlić I, Zou H, Zhang J, Li WX, Wang GT (2020) PhyloSuite: An integrated and scalable desktop platform for streamlined molecular sequence data management and evolutionary phylogenetics studies. Molecular Ecology Resources 20(1): 348–355. https://doi.org/10.1111/1755-0998.13096

Supplementary material 1

Figures S1–S100, Tables S1–S5

Authors: Blondelle Matio Kemkuignou, Lena Schweizer, Christopher Lambert, Elodie Gisèle M. Anoumedem, Simeon F. Kouam, Marc Stadler, Yasmina Marin-Felix

Data type: Docx file.

Explanation note: The following are available online: 1D, 2D NMR, ESIMS and HR-ESIMS spectra of compounds **1–13**; Fig S100, ML phylogram including our strain and type and reference strains of *Diaporthe* spp.; Table S1–S4, Information of the phylogenetic study; Alignment of the ITS, *cal*, *his3*, *tef1*, *tub2* sequences used in the second phylogenetic study.

Link: https://doi.org/10.3897/mycokeys.90.82871.suppl1